

A coupled-mode model for the hydroelastic analysis of large floating bodies over variable bathymetry regions

By K. A. BELIBASSAKIS AND G. A. ATHANASSOULIS

School of Naval Architecture and Marine Engineering, Section of Ship and Marine Hydrodynamics,
National Technical University of Athens, Heroon Polytechniou 9, Zografos 15773, Athens, Greece
kbel@fluid.mech.ntua.gr; mathan@central.ntua.gr

(Received 11 May 2004 and in revised form 7 December 2004)

The consistent coupled-mode theory (Athanasoulis & Belibassakis, *J. Fluid Mech.* vol. 389, 1999, p. 275) is extended and applied to the hydroelastic analysis of large floating bodies of shallow draught or ice sheets of small and uniform thickness, lying over variable bathymetry regions. A parallel-contour bathymetry is assumed, characterized by a continuous depth function of the form $h(x, y) = h(x)$, attaining constant, but possibly different, values in the semi-infinite regions $x < a$ and $x > b$. We consider the scattering problem of harmonic, obliquely incident, surface waves, under the combined effects of variable bathymetry and a floating elastic plate, extending from $x = a$ to $x = b$ and $-\infty < y < \infty$. Under the assumption of small-amplitude incident waves and small plate deflections, the hydroelastic problem is formulated within the context of linearized water-wave and thin-elastic-plate theory. The problem is reformulated as a transition problem in a bounded domain, for which an equivalent, Luke-type (unconstrained), variational principle is given. In order to consistently treat the wave field beneath the elastic floating plate, down to the sloping bottom boundary, a complete, local, hydroelastic-mode series expansion of the wave field is used, enhanced by an appropriate sloping-bottom mode. The latter enables the consistent satisfaction of the Neumann bottom-boundary condition on a general topography. By introducing this expansion into the variational principle, an equivalent coupled-mode system of horizontal equations in the plate region ($a \leq x \leq b$) is derived. Boundary conditions are also provided by the variational principle, ensuring the complete matching of the wave field at the vertical interfaces ($x = a$ and $x = b$), and the requirements that the edges of the plate are free of moment and shear force. Numerical results concerning floating structures lying over flat, shoaling and corrugated seabeds are presented and compared, and the effects of wave direction, bottom slope and bottom corrugations on the hydroelastic response are presented and discussed. The present method can be easily extended to the fully three-dimensional hydroelastic problem, including bodies or structures characterized by variable thickness (draught), flexural rigidity and mass distributions.

1. Introduction

The interaction of free-surface gravity waves with floating deformable bodies, in water of intermediate depth with a general bathymetry, is a mathematically interesting problem finding important applications. Very large floating structures (VLFS, megafloats) and platforms of shallow draught are examples of structures for which

hydroelastic effects are significant and should be properly taken into account. Such structures have been intensively studied, being under consideration for use as floating airports and mobile offshore bases. Extended surveys, including a literature review, have been recently presented by Kashiwagi (2000) and Watanabe, Utsunomiya & Wang (2004). Also, the hydroelastic analysis of floating bodies is relevant to problems concerning the interaction of water waves with ice sheets; an extended review can be found in Squire *et al.* (1995).

Although nonlinear effects are of specific importance, as e.g. in the study of significant local slamming phenomena, see e.g. Faltinsen (2001), Greco, Landrini & Faltinsen (2003), the solution of the linearized problem still provides valuable information, serving also as the basis for the development of weakly nonlinear models. The linearised problem associated with the hydroelastic responses of VLFS can be effectively treated in the frequency domain, and many methods have been developed for its solution. These include the B-spline Galerkin method by Kashiwagi (1998), boundary element methods (BEM) (Ertekin & Kim 1999; Hermans 2000; Hong, Choi & Hong 2001), hydroelastic eigenfunction expansion techniques (Kim & Ertekin 1998; Takagi, Shimada & Ikebuchi 2000; Hong *et al.* 2003), integro-differential equations (Adrianov & Hermans 2003), Wiener-Hopf techniques (Tkacheva 2001), Green–Naghdi models (Kim & Ertekin 2002), and others. Another approach, originally developed by Eatock Taylor & Waite (1978) and Bishop, Price & Wu (1986), and further extended by various authors, as e.g. Newman (1994), Wu, Watanabe & Utsunomiya (1995), is based on expressing the structure oscillations in a series expansion (using either dry elastic modes or another basis), identifying appropriate radiation problems and, finally, formulating and solving the coupled hydrodynamic equations. Meylan (2001) derived a variational equation for the plate–water system by expressing the water motion as an operator equation. In addition to the above, high-frequency asymptotic methods have been developed to describe the deflection dynamics of VLFS, see e.g. Ohkusu & Namba (1996), Hermans (2003). The latter are especially useful in the case of short waves interacting with a floating structure of large horizontal dimensions. Much information, as well as progress on VLFS, can be found in special issues of *J. Fluids Struct.* (Eatock Taylor & Ohkusu 2000) and *Mar. Struct.* (Ertekin *et al.* 2000, 2001), as well as in the VLFS sections of *ISOPE Conference Proceedings*.

Similar techniques have been developed for the interaction of water waves with ice sheets. For example, Marchenko & Shrira (1991), using Zakharov’s (1968) variational principle, developed a Hamiltonian formalism for the waves in the liquid beneath an ice sheet, and Meylan & Squire (1994) used Green’s function approach to formulate an integral equation over a floating plate. In the case of water-wave interaction with semi-infinite ice sheets, Balmforth & Craster (1999) used a Fourier transform approach in conjunction with Wiener–Hopf techniques, Linton & Chung (2003) developed a residue calculus technique, and Evans & Porter (2003) used eigenfunction expansion methods to study wave scattering by narrow cracks in ice sheets. A more thorough review concerning wave–ice interaction can be found in the above papers.

In most works dealing with the hydroelastic analysis of large floating bodies, the water depth has been assumed to be constant, either finite or infinite. This assumption cannot, in general, be justified in the case of (very) large floating bodies in nearshore and/or coastal waters. In this case, the variations of bathymetry over the extent of the floating body may be significant and might have important effects on the hydroelastic behaviour of the system; experimental evidence of these effects has been recently provided by Shiraiishi, Iijuma & Yoneyama (2002). Numerical methods for predicting the hydroelastic responses of VLFS in variable bathymetry regions have been recently

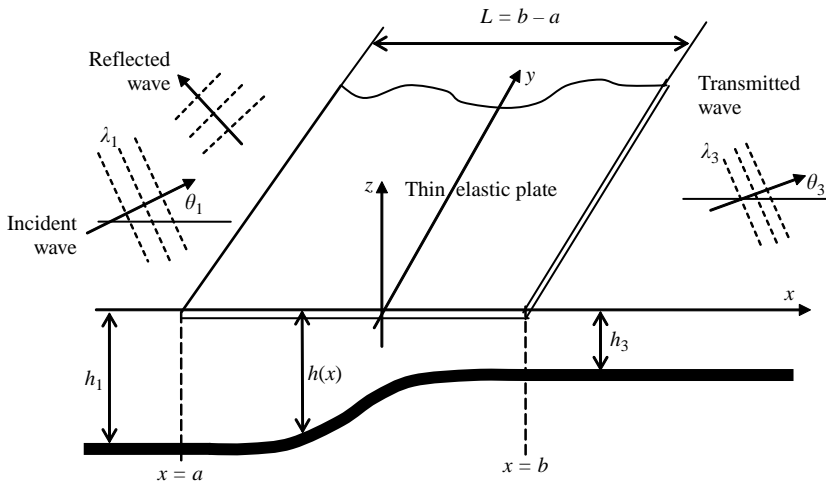


FIGURE 1. Floating elastic plate in variable bathymetry region.

proposed, based on BEM in conjunction with fast multipole techniques (Utsunomiya, Watanabe & Nishimura 2001), and on eigenfunction expansions in conjunction with a step-like bottom approximation (Murai, Inoue & Nakamura 2003). In addition, Porter & Porter (2004) have recently derived an approximate, vertically integrated, two-equation model for the problem of water-wave interaction with an ice sheet of variable thickness, lying over variable bathymetry, which is valid under mild-slope assumptions both with respect to the wetted surface of the ice sheet and the bottom boundary.

In the present work, a continuous coupled-mode technique is developed and applied to the hydroelastic analysis of large floating bodies of shallow draught or ice sheets of small and uniform thickness, lying over variable bathymetry regions. A parallel-contour bathymetry is assumed, characterized by a continuous depth function of the form $h(x, y) = h(x)$, attaining constant, but possibly different, values in the semi-infinite regions $x < a$ and $x > b$; see figure 1. We consider the scattering problem of harmonic, obliquely incident, surface waves, under the combined effects of variable bathymetry and a floating elastic plate, extending from $x = a$ to $x = b$ and $-\infty < y < \infty$. Under the assumption of small-amplitude incident waves and small plate deflections, the hydroelastic problem is formulated within the context of linearised water-wave and thin-elastic-plate theory. In contrast to the step-like bottom approximation, the present approach does not introduce artificial discontinuities (bottom corners). In order to consistently treat the wave field beneath the elastic floating plate, down to the sloping bottom boundary, an appropriate extension of the consistent coupled-mode theory, derived by Athanassoulis & Belibassakis (1999) and extended to three-dimensional by Belibassakis, Athanassoulis & Gerostathis (2001), has been developed and exploited. The present method is based on a complete, local, hydroelastic-mode series expansion of the wave field, enhanced by an appropriate sloping-bottom mode, enabling the consistent satisfaction of the Neumann bottom-boundary condition on a general topography. By introducing this expansion into an appropriate Luke-type variational principle (Luke 1967), an equivalent coupled-mode system of horizontal equations in the plate region ($a \leq x \leq b$) is derived. Unlike other Hamiltonian variational principles (see e.g. Marchenko & Shrira 1991; Nagata, Niizato & Ishiki 2002), constrained by the below-the-surface kinematics, the present one is totally unconstrained. Boundary

conditions are also provided by the variational principle, ensuring the complete matching of the wave field at the vertical interfaces ($x = a$ and $x = b$), and the requirements that the edges of the plate are free of moment and shear force.

The plan of our paper is as follows. In §2 the mathematical formulation of the problem is presented in the usual differential form, and in §3 the variational principle is given. The enhanced, local, hydroelastic-mode representation is introduced in §4. The latter, combined with the variational principle, leads to a coupled-mode system of horizontal equations with respect to the mode amplitudes and the elastic plate deflection, which is derived in §5. A selection of numerical examples, including comparisons with other methods, is presented and discussed in §6. In order to illustrate the effects of the bottom inhomogeneity, numerical results are presented concerning the deflection of large floating bodies lying over a flat bottom, a shoal and a corrugated seabed. With the aid of systematic comparisons, the effects of bottom slope and bottom corrugations on the hydroelastic response of large floating elastic plates are examined and discussed.

Future extensions and generalizations of the present method are directed towards: (i) the modelling of floating bodies with variable thickness, elastic parameters and mass distribution, also enabling application to the problem of wave interaction with ice sheets of general morphology, as e.g. described by Porter & Porter (2004); (ii) the solution of the fully three-dimensional problem over a general seafloor; and (iii) the modelling and analysis of the weakly nonlinear hydroelastic problem.

2. Differential formulation of the problem

The environment studied consists of a water layer D_{3D} bounded above partly by the free surface and partly by a large floating plate (large shallow-draught platform or ice sheet of uniform and small thickness), and below by a rigid bottom. It is assumed that the bottom surface exhibits an arbitrary one-dimensional variation in a subdomain of finite length, i.e. the bathymetry is characterized by straight and parallel bottom contours lying between two regions of constant but possibly different depth: $h = h_1$ (region of incidence) and $h = h_3$ (region of transmission); see figure 1. The slopes of both the liquid free surface $\tilde{\eta}(x, y; t)$ and the elastic-plate deflection $\tilde{w}(x, y; t)$ are assumed to be small enough that the standard linearised equations can be applied (see e.g. Stoker 1957 or Wehausen & Laitone 1960).

A Cartesian coordinate system is introduced, with its origin at some point on the mean elastic-plate surface (in the variable bathymetry region), the z -axis pointing upwards and the y -axis parallel to the bottom contours. The mean liquid domain is $D_{3D} = D \times R$, where D is the (two-dimensional) intersection of D_{3D} by a vertical plane perpendicular to the bottom contours, i.e. $D = \{(x, z) : x \in R, -h(x) < z < 0\}$, and $R = (-\infty, +\infty)$. The function $h(x)$, appearing in the above definitions, represents the local depth, measured from the mean water level. It is considered to be a smooth function of class C^2 defined on the real axis R , such that $h(x) = h(a) = h_1$, for all $x \leq a$, $h(x) = h(b) = h_3$, for all $x \geq b$.

The domain D is decomposed in three subdomains $D^{(i)}$, $i = 1, 2, 3$, defined as follows: $D^{(1)}$ is the constant-depth subdomain characterized by $x < a$ and constant depth h_1 ; $D^{(3)}$ is the constant-depth subdomain characterized by $x > b$ and constant depth h_3 ; and $D^{(2)}$ is the variable bathymetry subdomain, lying between $D^{(1)}$ and $D^{(3)}$, which also contains the floating elastic plate. The above decomposition is also applied to the free-surface/elastic-plate surface and bottom surface boundaries. Finally, we define the vertical interfaces separating the three subdomains, which are

vertical segments (between the bottom and the mean water level) at $x = a$ and $x = b$, respectively, shown by dashed lines in figure 1.

We consider the scattering problem of harmonic, obliquely incident, surface (gravity) plane waves of angular frequency ω , under the combined effects of variable bathymetry and a semi-infinite (along the y -direction) thin floating elastic plate extending from $x = a$ to $x = b$. The waves propagate with directions θ_1 and θ_3 with respect to the x -axis in the regions of incidence ($x \leq a$) and transmission ($x \geq b$), respectively. Under the usual assumptions of linearised water-wave theory and thin-elastic-plate theory, the problem can be treated by partial separation of variables with respect to the transverse y -coordinate. The wave potential can be expressed in the form

$$\tilde{\Phi}(x, y, z; t) = \text{Re} \left(-\frac{igH}{2\omega} \varphi(x, z) \exp(i(qy - \omega t)) \right), \tag{2.1a}$$

where H is the incident wave height, g is the acceleration due to gravity, and $i = \sqrt{-1}$. (The constant q is related with the y -periodicity of the fields and will be defined later.) The liquid free-surface elevation is expressed in terms of the wave potential by using the linearised Bernoulli's equation on the free surface,

$$\tilde{\eta}(x, y; t) = -\frac{1}{g} \frac{\partial \tilde{\Phi}(x, y, z = 0; t)}{\partial t} = \text{Re} \left(\frac{H}{2} \varphi(x, z = 0) \exp(i(qy - \omega t)) \right). \tag{2.1b}$$

The elastic-plate deflection is connected to the wave potential by means of the linearised kinematical condition at the liquid–solid interface,

$$\frac{\partial \tilde{w}(x, y; t)}{\partial t} = \frac{\partial \tilde{\Phi}(x, y, z = 0; t)}{\partial z},$$

which reduces to

$$\tilde{w}(x, y; t) = \text{Re}(w(x) \exp(i(qy - \omega t))), \quad \text{where} \quad w(x) = \frac{i}{\omega} \frac{\partial \varphi(x, z = 0)}{\partial z}, \tag{2.1c}$$

in the frequency domain. The constant

$$q = \kappa_0^{(1)} \sin \theta_1 \tag{2.2}$$

denotes the periodicity constant along the y -direction, which is determined by the wave number $\kappa_0^{(1)} = 2\pi/\lambda_1$ of the incident wave and its direction of propagation θ_1 in the region $D^{(1)}$, far from the elastic plate and the bottom irregularity ($x \rightarrow -\infty$). The direction of the transmitted wave in the region $D^{(3)}$ ($x \rightarrow \infty$) is given by (see also Massel 1993),

$$\theta_3 = \sin^{-1} (\kappa_0^{(1)} \sin \theta_1 / \kappa_0^{(3)}), \tag{2.3}$$

where $\kappa_0^{(3)} = 2\pi/\lambda_3$ is the wavenumber of the transmitted wave. Energy conservation leads to the equation (Wehausen & Laitone 1960, §17; Massel 1993):

$$c_g^{(1)}(1 - |A_R|^2) \cos \theta_1 = c_g^{(3)} |A_T|^2 \cos \theta_3, \tag{2.4}$$

where A_R is the reflection coefficient and A_T is the transmission coefficient (defined as the ratios of the corresponding wave amplitudes to the incident wave amplitude), and

$$c_g^{(j)} = \frac{\omega}{2\kappa_0^{(j)}} \left(1 + \frac{2\kappa_0^{(j)} h_j}{\sinh(2\kappa_0^{(j)} h_j)} \right), \quad j = 1, 3, \tag{2.5}$$

are the group velocities in the left ($D^{(1)}$) and right ($D^{(3)}$) half-strips. Equation (2.4) imposes a constraint between the wave parameters at infinity and can be used for checking the accuracy of any numerical solution. The problem of water-wave scattering by the elastic plate, with the effects of variable bathymetry, can be formulated as a transmission problem in the bounded subdomain $D^{(2)} = \{(x, z) : -h(x) < z < 0, a < x < b\}$ with the aid of the following general representations of the complex wave potential $\varphi(x, z)$ in the two semi-infinite strips $D^{(1)} = \{(x, z) : -h_1 < z < 0, -\infty < x < a\}$ and $D^{(3)} = \{(x, z) : -h_3 < z < 0, b < x < \infty\}$ (see e.g. Kirby & Dalrymple 1983; Massel 1993):

$$\begin{aligned} \varphi^{(1)}(x, z) = & (\exp(ik_0^{(1)}x) + A_R \exp(-ik_0^{(1)}x))Z_0^{(1)}(z) \\ & + \sum_{n=1}^{\infty} C_n^{(1)}Z_n^{(1)}(z) \exp(k_n^{(1)}(x-a)) \quad \text{in } D^{(1)}, \end{aligned} \quad (2.6a)$$

$$\varphi^{(3)}(x, z) = A_T \exp(ik_0^{(3)}x)Z_0^{(3)}(z) + \sum_{n=1}^{\infty} C_n^{(3)}Z_n^{(3)}(z) \exp(k_n^{(3)}(b-x)) \quad \text{in } D^{(3)}. \quad (2.6b)$$

In the series (2.6a, b), the terms

$$(\exp(ik_0^{(1)}x) + A_R \exp(-ik_0^{(1)}x))Z_0^{(1)}(z) \quad \text{and} \quad A_T \exp(ik_0^{(3)}x)Z_0^{(3)}(z)$$

are the *propagating modes*, while the remaining ones ($n = 1, 2, \dots$) are the *evanescent modes*. In the above expansions, the quantities

$$k_0^{(j)} = \sqrt{(\kappa_0^{(j)})^2 - q^2}, \quad k_n^{(j)} = \sqrt{(\kappa_n^{(j)})^2 + q^2}, \quad n = 1, 2, 3, \dots, \quad j = 1, 3, \quad (2.7a)$$

are horizontal wavenumbers, which are defined in terms of the eigenvalues $\{ik_0^{(j)}, \kappa_n^{(j)}, n = 1, 2, \dots\}$ of the associated vertical Sturm–Liouville problems, obtained as the roots of the dispersion relations

$$\mu h_j = -\kappa^{(j)} h_j \tan(\kappa^{(j)} h_j), \quad \mu = \omega^2/g, \quad j = 1, 3. \quad (2.7b)$$

Finally, the functions $\{Z_n^{(j)}(z), n = 0, 1, 2, \dots\}$, appearing in (2.6a, b), denote the corresponding eigenfunctions, and are given by

$$Z_0^{(j)}(z) = \frac{\cosh(\kappa_0^{(j)}(z + h_j))}{\cosh(\kappa_0^{(j)} h_j)}, \quad Z_n^{(j)}(z) = \frac{\cos(\kappa_n^{(j)}(z + h_j))}{\cos(\kappa_n^{(j)} h_j)},$$

$$n = 1, 2, \dots, \quad j = 1, 3. \quad (2.8)$$

Using the representations (2.6a, b), for the wave potential in the two half-strips $D^{(1)}$ and $D^{(3)}$, in conjunction with the linearised water-wave equations in $D^{(2)}$, and the standard thin-plate theory (see e.g. Magrab 1979), the hydroelastic problem examined is reformulated as follows:

Find the fields $w(x)$, $a \leq x \leq b$, and $\varphi^{(2)}(x, z) = \varphi(x, z)$, in the bounded subdomain $D^{(2)} = \{(x, z) : -h(x) < z < 0, a < x < b\}$, satisfying the following differential equations, boundary and matching conditions:

$$(\nabla^2 - q^2)\varphi^{(2)} = 0 \quad \text{in } -h(x) < z < 0, \quad a < x < b, \quad (2.9a)$$

$$D\left(\left(\frac{\partial^2}{\partial x^2} - q^2\right)^2 w\right) + (1 - \varepsilon)w - \frac{i\mu}{\omega}\varphi^{(2)} = 0 \quad \text{on } z = 0, \quad a < x < b, \quad (2.9b)$$

$$w = \frac{i}{\omega} \frac{\partial \varphi^{(2)}}{\partial z} \quad \text{on } z = 0, \quad a < x < b, \quad (2.9c)$$

$$\frac{\partial \varphi^{(2)}}{\partial z} + \frac{dh}{dx} \frac{\partial \varphi^{(2)}}{\partial z} = 0 \quad \text{on } z = -h(x), \quad a < x < b, \quad (2.9d)$$

$$\varphi^{(2)} = \varphi^{(1)}, \quad \frac{\partial \varphi^{(2)}}{\partial x} = \frac{\partial \varphi^{(1)}}{\partial x} \quad \text{on } x = a, \quad -h_1 < z < 0, \quad (2.9e)$$

$$\varphi^{(2)} = \varphi^{(3)}, \quad \frac{\partial \varphi^{(2)}}{\partial x} = \frac{\partial \varphi^{(3)}}{\partial x} \quad \text{on } x = b, \quad -h_3 < z < 0, \quad (2.9f)$$

$$\frac{\partial^3 w}{\partial x^3} - (2 - \nu)q^2 \frac{\partial w}{\partial x} = 0 \quad \text{at } x = a, z = 0 \quad \text{and at } x = b, z = 0, \quad (2.9g)$$

$$\frac{\partial^2 w}{\partial x^2} - \nu q^2 w = 0 \quad \text{at } x = a, z = 0 \quad \text{and at } x = b, z = 0. \quad (2.9h)$$

Equation (2.9a) is the modified Helmholtz equation on the x, z vertical plane, which reduces to the Laplace equation in the case of normal incidence $\theta_1 = 0$; cf. (2.2). The boundary condition (2.9b) describes the coupled dynamics of the thin elastic plate (modelling the floating structure) and the underlying fluid flow; see e.g. Meylan & Squire (1994) or Andrianov & Hermans (2003). It is obtained by combining the thin-elastic-plate equation with the linearised Bernoulli's equation on the mean elastic plate surface ($z = 0$), and involves the (constant) parameters $D = \hat{D}/\rho g$ and $\varepsilon = m\omega^2/\rho g$, where $\hat{D} = Et^3/12(1 - \nu^2)$ denotes the flexural rigidity of the elastic plate (the equivalent flexural rigidity of the platform), and m is the mass per unit area of the plate. Moreover, ρ denotes the fluid density and $\mu = \omega^2/g$ is the frequency parameter. Equations (2.9c, d) are the kinematic conditions on the liquid–solid interface and the seabed, respectively. Equations (2.9e, f) are matching conditions on the vertical interfaces at $x = a$ and $x = b$, separating the three subdomains. Finally, the edge conditions (2.9g, h) state that the ends ($x = a$ and $x = b$) of the plate are free of shear force and moment, where ν denotes Poisson's ratio.

3. Variational formulation

The problem (2.9a–h) admits an unconstrained variational formulation, which will serve as the basis for the derivation of an equivalent coupled-mode system of equations on the horizontal plane. We consider the functional:

$$\begin{aligned} & F(\varphi^{(2)}(x, z), w(x), A_R, \{C_n^{(1)}\}_{n \in N}, A_T, \{C_n^{(3)}\}_{n \in N}) \\ &= \frac{\mu}{2} \int_{x=a}^{x=b} \int_{z=-h(x)}^{z=0} ((\nabla \varphi^{(2)})^2 + (q\varphi^{(2)})^2) dz dx + i\omega\mu \int_{x=a}^{x=b} \varphi^{(2)} w dx \\ &\quad - \frac{\omega^2 D}{2} \int_{x=a}^{x=b} \left(\left(\frac{\partial^2 w}{\partial x^2} \right)^2 + 2q^2 \left(\frac{\partial w}{\partial x} \right)^2 + \left(q^4 + \frac{1-\varepsilon}{D} \right) w^2 \right) dx + \nu\omega^2 D q^2 \left[w \frac{\partial w}{\partial x} \right]_{x=a}^{x=b} \\ &\quad + \mu \int_{z=-h_1}^{z=0} \left(\varphi^{(2)} - \frac{1}{2} \varphi^{(1)}(A_R, \{C_n^{(1)}\}_{n \in N}) \right) \frac{\partial \varphi^{(1)}(A_R, \{C_n^{(1)}\}_{n \in N})}{\partial x} dz \\ &\quad - \mu \int_{z=-h_3}^{z=0} \left(\varphi^{(2)} - \frac{1}{2} \varphi^{(3)}(A_T, \{C_n^{(3)}\}_{n \in N}) \right) \frac{\partial \varphi^{(3)}(A_T, \{C_n^{(3)}\}_{n \in N})}{\partial x} dz - \mu A_0 A_R J^{(1)}, \end{aligned} \quad (3.1)$$

where

$$J^{(1)} = 2k_0^{(1)} \int_{z=-h_1}^{z=0} (Z_0^{(1)}(z))^2 dz.$$

The arguments of the functional F , which express the degrees of freedom of the coupled hydroelastic system are: the wave potential $\varphi^{(2)}(x, z)$, $(x, z) \in D^{(2)}$, the elastic-plate deflection $w(x)$, $a \leq x \leq b$, and the coefficients A_R , $\{C_n^{(1)}\}_{n \in N}$ and A_T , $\{C_n^{(3)}\}_{n \in N}$, which enter the principle through the representations (2.6a, b) of the half-strip wave potentials $\varphi^{(1)}$ and $\varphi^{(3)}$. The coefficients A_R , $\{C_n^{(1)}\}_{n \in N}$ and A_T , $\{C_n^{(3)}\}_{n \in N}$ control the liquid dynamics in the two half-strips, ensuring full dynamical coupling between the three regions $D^{(j)}$, $j = 1, 2, 3$. As shown in the Appendix, the variational equation based on the part of the above functional that consists of the first, second, third and fifth terms under the integral on the mean plate surface (third term on the right-hand side of (3.1)) and of the end terms (fourth term on the right-hand side of (3.1)) is equivalent to the variational equation based on the standard energy functional of the thin-plate theory, that is defined as the difference between the strain energy of the plate and the kinetic energy of the plate; see e.g. Magrab (1979, equation 6.20).

In terms of functional (3.1), the hydroelastic problem (2.9a–h) is reformulated as a variational problem of the form

$$\delta F(\varphi^{(2)}, w, A_R, \{C_n^{(1)}\}, A_T, \{C_n^{(3)}\}) = 0. \tag{3.2}$$

To establish the above variational principle, we have to calculate the first variation δF of the functional (3.1); see e.g. Mei (1983, §4.11). Making use of Green’s theorem and the properties of the modal representations (2.6a, b) in the semi-infinite strips $D^{(1)}$, $D^{(3)}$, and applying appropriate integration by parts to the term containing the integral on the plate surface (third term on the right-hand side of (3.1)), the above variational equation, finally, takes the form:

$$\begin{aligned} & \mu \int_{x=a}^{x=b} \int_{z=-h(x)}^{z=0} (\nabla^2 - q^2)\varphi^{(2)}\delta\varphi^{(2)} \, dz \, dx + \mu \int_{x=a}^{x=b} \left(\frac{\partial\varphi^{(2)}}{\partial z} + \frac{dh}{dx} \frac{\partial\varphi^{(2)}}{\partial x} \right) \delta\varphi^{(2)} \Big|_{z=-h(x)} \, dx \\ & - \mu \int_{x=a}^{x=b} \left(i\omega w + \frac{\partial\varphi^{(2)}}{\partial z} \right) \delta\varphi^{(2)} \Big|_{z=0} \, dx + \omega^2 \int_{x=a}^{x=b} \left(D \left(\frac{\partial^2}{\partial x^2} - q^2 \right)^2 w + (1 - \varepsilon)w \right. \\ & \left. - \frac{i\mu}{\omega} \varphi^{(2)} \Big|_{z=0} \right) \delta w \, dx + \mu \int_{z=-h_1}^{z=0} \left(\frac{\partial\varphi^{(2)}}{\partial x} - \frac{\partial\varphi^{(1)}}{\partial x} \right) \delta\varphi^{(2)} \Big|_{x=a} \, dz \\ & - \mu \int_{z=-h_1}^{z=0} (\varphi^{(2)} - \varphi^{(1)}) \delta \left(\frac{\partial\varphi^{(1)}}{\partial x} \right) \Big|_{x=a} \, dz - \mu \int_{z=-h_3}^{z=0} \left(\frac{\partial\varphi^{(2)}}{\partial x} - \frac{\partial\varphi^{(3)}}{\partial x} \right) \delta\varphi^{(2)} \Big|_{x=b} \, dz \\ & + \mu \int_{z=-h_3}^{z=0} (\varphi^{(2)} - \varphi^{(3)}) \delta \left(\frac{\partial\varphi^{(3)}}{\partial x} \right) \Big|_{x=b} \, dz - \omega^2 D \left[\left(\frac{\partial^3 w}{\partial x^3} - (2 - \nu)q^2 \frac{\partial w}{\partial x} \right) \delta w \right]_{x=a}^{x=b} \\ & + \omega^2 D \left[\left(\frac{\partial^2 w}{\partial x^2} - \nu q^2 w \right) \delta \left(\frac{\partial w}{\partial x} \right) \right]_{x=a}^{x=b} = 0. \end{aligned} \tag{3.3}$$

The proof of the equivalence of the variational equation (3.3) and the hydroelastic problem (2.9a–h) is obtained by using standard arguments of the *Calculus of Variations*. The independent variations in (3.3) are: (i) $\delta\varphi^{(2)}$ in $D^{(2)}$, (ii) $\delta\varphi^{(2)}$ on the bottom surface $z = -h(x)$, (iii) $\delta\varphi^{(2)}$ on the mean plate surface $z = 0$, (iv) $\delta\varphi^{(2)}$ on the vertical interfaces at $x = a$ and $x = b$, (v) δA_R , $\{\delta C_n^{(1)}\}_{n \in N}$, δA_T , $\{\delta C_n^{(3)}\}_{n \in N}$ entering through the variations $\delta(\partial\varphi^{(j)}/\partial x)$, $j = 1, 3$, at $x = a$ and $x = b$, respectively, (vi) δw in $a < x < b$, (vii) δw at the end points $x = a$ and $x = b$, and (viii) $\delta(\partial w/\partial x)$ at $x = a$ and $x = b$.

The variational principle (3.3) is totally unconstrained, in the sense that all equations (2.9a–h) are obtained as natural conditions, the only requirements imposed on the admissible function spaces being some plausible smoothness assumptions concerning

$\varphi^{(2)}(x, z)$ in $D^{(2)}$ and $w(x)$ in $a \leq x \leq b$. (This turns to be a non-trivial requirement on the non-horizontal part of the seabed, as we shall see in the next section.)

4. Enhanced local hydroelastic-mode series expansion

The problem of determining $\varphi^{(2)}(x, z)$ in $D^{(2)}$, satisfying the variational principle (3.3), will be treated by an appropriate extension of the consistent coupled-mode theory developed by Athanassoulis & Belibassakis (1999), for water-wave propagation in variable bathymetry regions. We first review the vertical eigenfunction expansion of the solution to the hydroelastic problem (2.9a–h) in the constant-depth case, $h(x) = h = \text{const}$. As shown by various authors (e.g. Kim & Ertekin 1998; Takagi *et al.* 2000; Hong *et al.* 2003), in this case, separation of variables is possible, leading to an expansion of the form

$$\varphi^{(2)}(x, z) = \sum_{n=0}^{\infty} \varphi_n(x) Z_n(z), \quad -h < z < 0, \quad a < x < b. \tag{4.1}$$

In the above equation, the term $\varphi_0(x) Z_0(z)$ corresponds to the *propagating mode*, the terms $\varphi_n(x) Z_n(z), n = 1, 2$, correspond to the *decaying-propagating modes*, and the remaining terms $\varphi_n(x) Z_n(z), n = 3, 4, \dots$, express the *evanescent modes*, which are especially important in the vicinity of the two edges $x = a$ and $x = b$. The functions $Z_n(z), n \geq 0$, appearing in (4.1), are obtained as the eigenfunctions of the following vertical *Steklov-type eigenvalue* problem:

$$\frac{d^2 Z_n(z)}{dz^2} - \kappa_n^2 Z_n(z) = 0 \quad \text{in the interval } -h < z < 0, \tag{4.2a}$$

$$\frac{dZ_n(z = -h)}{dz} = 0 \quad \text{at the bottom } z = -h, \tag{4.2b}$$

$$(D\kappa_n^4 - \varepsilon + 1) \frac{dZ_n(z = 0)}{dz} - \mu Z_n(z = 0) = 0 \quad \text{at the interface } z = 0. \tag{4.2c}$$

The solution of the above problem is given by

$$Z_n(z) = \frac{\cosh[\kappa_n(z + h)]}{\cosh(\kappa_n h)}, \quad n = 0, 1, 2, 3, \dots, \tag{4.3a}$$

where the eigenvalues $\{\kappa_n, n = 0, 1, 2, \dots\}$ are obtained as the roots of the dispersion relation

$$\mu = (D\kappa^4 + 1 - \varepsilon) \kappa \tanh(\kappa h), \tag{4.3b}$$

which are distributed on the complex plane as shown in figure 2. Only the symmetric subset of the roots of (4.3b), shown in figure 2 by open circles, is needed in the expansion (4.1).

The indexing of the roots of (4.3b) is as follows: κ_0 is the real-positive root, κ_1 is the root inside the first quadrant of the complex plane (i.e. $\text{Re}(\kappa_1) > 0, \text{Im}(\kappa_1) > 0$), κ_2 is the conjugate-symmetric of κ_1 (thus, $\kappa_2 = -\text{Re}(\kappa_1) + i \text{Im}(\kappa_1)$), and $\kappa_n, n = 3, 4, 5, \dots$ are the roots lying on the positive-imaginary axis ($\text{Im}(\kappa_n) > 0$). The wave potential $\varphi^{(2)}(x, z)$, as defined through (4.1), identically satisfies the flat bottom boundary condition $\partial\varphi^{(2)}(x, z = -h)/\partial z = 0$, since each term in the expansion does. Moreover, the modal amplitudes $\varphi_n(x), n = 0, 1, 2, \dots$, should satisfy the uncoupled horizontal equations

$$\varphi_m''(x) + (\kappa_m^2 - q^2)\varphi_m(x) = 0, \quad m = 0, 1, 2, 3, \dots, \tag{4.4}$$

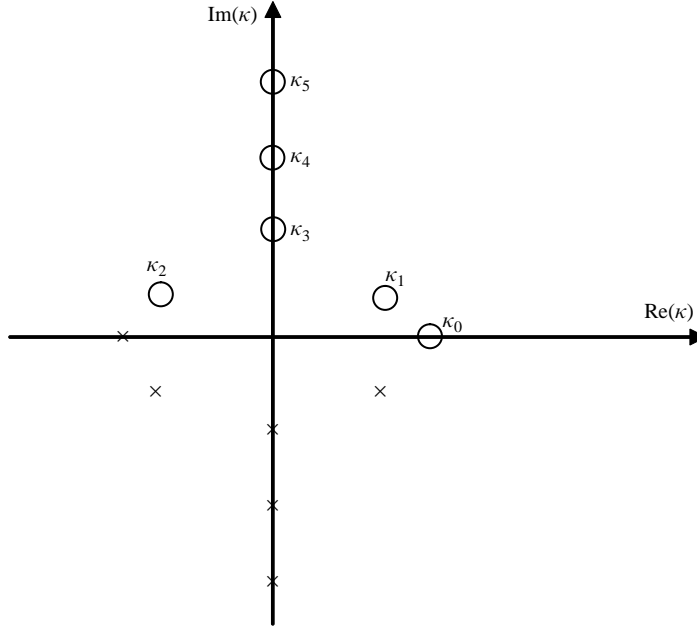


FIGURE 2. Distribution of the roots of (4.3b) on the complex κ -plane.

derived by separation of variables from the modified Helmholtz equation (or the Laplace equation, for $q = 0$). Combining (4.4) with (4.2a–c) and the dispersion relation (4.3b), and using (2.9c) to eliminate $w(x)$, we easily see that each term of the expansion (4.1) also satisfies the liquid–plate interface condition (2.9b). Recapitulating, we can make the statement that, in constant depth, the eigenfunction expansion (4.1) satisfies all three equations (2.9a), (2.9b) and (2.9d), with the proviso that $\varphi_n(x)$, $n = 0, 1, 2, \dots$, satisfy (4.4). The completeness of the expansion (4.1), in the space of functions satisfying the same conditions as the set of eigenfunctions $\{Z_n(z), n = 0, 1, 2, \dots\}$, both at the flat bottom, (4.2b), and at the fluid–solid interface, (4.2c), has been recently demonstrated by Evans & Porter (2003, § 4).

We shall now proceed to generalize the eigenfunction expansion (4.1) to the variable bathymetry case. This will be done along the lines of the works by Athanassoulis & Belibassakis (1999), Belibassakis *et al.* (2001), Athanassoulis & Belibassakis (2002). When the bottom surface is varying ($h'(x) \neq 0$), the vertical eigenfunction problem (4.2a–c) becomes parametrically dependent on x , since the bottom boundary condition is now applied to $z = -h(x)$. The completeness property of the system $\{Z_n(z; x), n = 0, 1, 2, \dots\}$ suggests a first generalization of (4.1) in the form

$$\varphi^{(2)}(x, z) = \sum_{n=0}^{\infty} \varphi_n(x) Z_n(z; x), \quad -h(x) < z < 0, \quad a < x < b, \quad (4.5a)$$

where

$$Z_n(z; x) = \frac{\cosh[\kappa_n(x)(z + h(x))]}{\cosh(\kappa_n(x)h(x))}, \quad n = 0, 1, 2, 3, \dots, \quad (4.5b)$$

and the x -dependent eigenvalues $\{\kappa_n(x), n = 0, 1, 2, \dots\}$ are obtained as the roots of the (local) dispersion relation

$$\mu = (D\kappa^4(x) + 1 - \varepsilon)\kappa(x) \tanh(\kappa(x)h(x)), \quad a < x < b. \quad (4.5c)$$

The functions $Z_n(z; x), n = 0, 1, 2 \dots$, are formally obtained as the eigenfunctions of the *local vertical eigenvalue* problem of the form (4.2a-c), formulated at the local depth $h(x)$, for each x in the interval $a \leq x \leq b$.

There is, however, an apparent incompatibility between the expansion $\sum_{n=0}^{\infty} \varphi_n(x) \cdot Z_n(z; x)$, all terms of which satisfy the condition $\partial Z_n(z = -h(x); x) / \partial z = 0$, for all x in the interval $a \leq x \leq b$, and the field sought $\varphi^{(2)}(x, z)$, which must satisfy $\partial \varphi^{(2)}(x, z = -h(x)) / \partial z \neq 0$, at those x in $a \leq x \leq b$ where the seabed is non-horizontal ($h'(x) \neq 0$). This fact has also the consequence that the series (4.5a) converges poorly in variable bathymetry regions.

The key idea to overcome this incompatibility, which has been analysed by the present authors in a series of papers mentioned above, is to subtract from the field sought $\varphi^{(2)}(x, z)$ an appropriate function $\varphi_{-1}(x, z)$, so that the difference $f(x, z) = \varphi^{(2)}(x, z) - \varphi_{-1}(x, z)$ satisfies the same condition at the sloping bottom, $\partial f(x, z = -h(x)) / \partial z = 0$, as the system $\{Z_n(z; x), n = 0, 1, 2 \dots\}$ does. The latter field $f(x, z)$ is then expanded in terms of the local eigenfunctions $Z_n(z; x), n = 0, 1, 2 \dots$, providing us with a consistent representation of the form

$$f(x, z) = \varphi^{(2)}(x, z) - \varphi_{-1}(x, z) = \sum_{n=0}^{\infty} \varphi_n(x) Z_n(z; x).$$

The additional term $\varphi_{-1}(x, z)$ is also represented in the form $\varphi_{-1}(x, z) = \varphi_{-1}(x) Z_{-1}(z; x)$, where $Z_{-1}(z; x)$ is an appropriate vertical profile (explained below) and $\varphi_{-1}(x)$ is an additional mode-amplitude, which will be called the *sloping-bottom mode*, accounting for the satisfaction of the bottom boundary condition on the sloping parts of the bottom. Thus, the following *enhanced local-mode representation* is derived

$$\varphi^{(2)}(x, z) = \varphi_{-1}(x) Z_{-1}(z; x) + \sum_{n=0}^{\infty} \varphi_n(x) Z_n(z; x), \quad -h(x) < z < 0, \quad a < x < b. \quad (4.6)$$

In contrast to the set of functions $Z_n(z; x), n = 0, 1, 2, 3 \dots$, which all satisfy $\partial Z_n(z = -h(x); x) / \partial z = 0$ on the bottom $z = -h(x)$, the term $Z_{-1}(z; x)$ is taken to be a smooth z -function satisfying the following inhomogeneous condition on the seabed:

$$\frac{\partial Z_{-1}(z = -h(x); x)}{\partial z} = 1. \quad (4.7a)$$

Equation (4.7a), in conjunction with representation (4.6) after a termwise z -differentiation, leads to the following interpretation of the amplitude of the sloping-bottom mode:

$$\varphi_{-1}(x) = \frac{\partial \varphi^{(2)}(x, z = -h(x))}{\partial z}. \quad (4.7b)$$

A consequence of (4.7b) is that the sloping-bottom term $\varphi_{-1}(x) Z_{-1}(z; x)$ identically vanishes on the horizontal parts ($h'(x) = 0$) of the bottom.

To derive a condition for $Z_{-1}(z; x)$ on the fluid-solid interface ($z = 0$), we consider the corresponding boundary condition (2.9b) on $z = 0$, expressed in terms of the wave potential $\varphi^{(2)}(x, z)$ (using (2.9c) to eliminate w):

$$D \left(\left(\frac{\partial^2}{\partial x^2} - q^2 \right)^2 \frac{\partial \varphi^{(2)}}{\partial z} \right) + (1 - \varepsilon) \frac{\partial \varphi^{(2)}}{\partial z} - \mu \varphi^{(2)} = 0 \quad \text{on } z = 0, \quad a < x < b.$$

Using (2.9a) at $z=0$ to replace the horizontal derivatives of $\varphi^{(2)}(x, z)$ by the corresponding vertical derivatives in the above equation, we find that

$$D \frac{\partial^5 \varphi^{(2)}}{\partial z^5} + (1 - \varepsilon) \frac{\partial \varphi^{(2)}}{\partial z} - \mu \varphi^{(2)} = 0 \quad \text{on } z = 0, \quad a < x < b \quad (4.8a)$$

that is the same condition as the one satisfied by each $Z_n(z; x)$, $n = 0, 1, 2, \dots$, at $z = 0$ (cf. (4.5c)). Thus, the extra sloping-bottom mode $\varphi_{-1}(x)Z_{-1}(z; x)$ should also satisfy (4.8a), resulting in

$$D \frac{\partial^5 Z_{-1}}{\partial z^5} + (1 - \varepsilon) \frac{\partial Z_{-1}}{\partial z} - \mu Z_{-1} = 0 \quad \text{at } z = 0 \quad \text{and for } a < x < b. \quad (4.8b)$$

The last requirement makes the sloping-bottom mode $\varphi_{-1}(x)Z_{-1}(z; x)$ compatible with the rest of the modes on $z = 0$. Thus, the representation (4.6) is compatible with both the bottom boundary condition (2.9d), as well as with the fluid–solid interface boundary condition (2.9b), with the proviso that the modified Helmholtz (or Laplace) equation is satisfied. A specific convenient form of $Z_{-1}(z; x)$ is given by

$$Z_{-1}(z; x) = h(x) \left[\left(\frac{z}{h(x)} \right)^3 + \left(\frac{z}{h(x)} \right)^2 \right], \quad (4.9)$$

and all results presented in this work are based on the above choice, although other choices are also possible. However, extensive numerical experimentation with other possible choices has proven that the final solution concerning the wave potential, as obtained by the enhanced representation (4.6), always remains the same for all valid forms of $Z_{-1}(z; x)$.

More details about the role and significance of the sloping-bottom mode can be found in Athanassoulis & Belibassakis (1999, §4), where this concept was first introduced for developing a consistent coupled-mode system for water-wave propagation over variable bathymetry regions, which is not restricted by any mild-slope assumption concerning the bottom profile.

5. The coupled-mode system of equations

By introducing the series representations (2.6a), (4.6) and (2.6b) for the potentials $\varphi^{(j)}(x, z)$, $j = 1, 2, 3$, in the variational principle (3.3), and expressing all variations in terms of $\delta\varphi_n(x)$, $n = -1, 0, 1, 2, \dots$, and δA_R , $\{\delta C_n^{(1)}\}_{n \in N}$, δA_T , $\{\delta C_n^{(3)}\}_{n \in N}$, it is possible to obtain a coupled-mode system (CMS) of horizontal differential equations for $\varphi_n(x)$ and $w(x)$, along with the appropriate boundary conditions at the end points $x = a$ and $x = b$. The derivation can be made by following exactly the same procedure as in Athanassoulis & Belibassakis (1999).

5.1. The CMS in the case of variable bathymetry

The first three terms on the left-hand side of variational equation (3.3) (that is the integrals over $D^{(2)}$, the seabed $z = -h(x)$ and the liquid-plate interface $z = 0$), result in the following second-order coupled-mode system of ordinary differential equations with respect to $\varphi_n(x)$:

$$\sum_{n=-1}^{\infty} a_{mn}(x) \frac{\partial^2 \varphi_n}{\partial x^2}(x) + b_{mn}(x) \frac{\partial \varphi_n}{\partial x} + c_{mn}(x) \varphi_n(x) = i\omega\mu w(x), \quad m = -1, 0, 1, \dots, \quad (5.1a)$$

while from the fourth term of (3.3) we obtain the fourth-order equation with respect to $w(x)$:

$$D \left(\frac{\partial^2}{\partial x^2} - q^2 \right)^2 w + (1 - \varepsilon)w = \frac{i\mu}{\omega} \sum_{n=-1}^{\infty} \varphi_n(x), \tag{5.1b}$$

both in $a < x < b$. The x -dependent coefficients of the CMS (5.1a, b) are

$$a_{mn}(x) = \mu \langle Z_n, Z_m \rangle, \tag{5.2a}$$

$$b_{mn}(x) = 2\mu \left\langle \frac{\partial Z_n}{\partial x}, Z_m \right\rangle + \mu \frac{dh}{dx} Z_n(z = -h; x) Z_m(z = -h; x), \tag{5.2b}$$

$$c_{mn}(x) = \mu \left\langle \frac{\partial^2 Z_n}{\partial x^2} + \frac{\partial^2 Z_n}{\partial z^2} - q^2 Z_n, Z_m \right\rangle - \mu \frac{\partial Z_n(z = 0; x)}{\partial z} Z_m(z = 0; x) + \mu \left(\frac{\partial Z_n(z = -h; x)}{\partial z} + \frac{dh}{dx} \frac{\partial Z_n(z = -h; x)}{\partial x} \right) Z_m(z = -h; x), \tag{5.2c}$$

where

$$\langle f, g \rangle = \int_{z=-h(x)}^{z=0} f(z)g(z) dz.$$

It is interesting to note that the coefficients $b_{mn}(x)$ and $c_{mn}(x)$, (5.2b, c), are defined in terms of both z -integrals (coming from the first term on the left-hand side of (3.3) and denoted by $\langle \cdot, \cdot \rangle$) and surface values of the functions Z_n and their derivatives at $z = 0$ and/or $z = -h(x)$.

Calculating the fifth and sixth terms on the left-hand side of (3.3), i.e. the integrals on the vertical interface at $x = a$, we obtain relations between the coefficients $A_R, \{C_n^{(1)}\}_{n \in N}$ and the values $\varphi_n(a)$ and $\varphi'_n(a)$, $n = 0, 1, 2, \dots$, where a prime denotes differentiation with respect to x . Similarly, calculating the seventh and eight terms in (3.3), i.e. the integrals on the vertical interface at $x = b$, we obtain relations between the coefficients $A_T, \{C_n^{(3)}\}_{n \in N}$ and the values $\varphi_n(b)$ and $\varphi'_n(b)$, $n = 0, 1, 2, \dots$. Eliminating the coefficients $A_R, \{C_n^{(1)}\}_{n \in N}, A_T, \{C_n^{(3)}\}_{n \in N}$ from these relations, we obtain the following boundary conditions, which are equivalent to the matching of the wave field at the vertical interfaces:

$$\sum_{n=0}^{\infty} (\varphi'_n(a) + ik_0^{(1)} \varphi_n(a)) B_{n0}^{(1)} = 2ik_0^{(1)} \exp(ik_0^{(1)} a) \|Z_0^{(1)}\|^2, \tag{5.3a}$$

$$\sum_{n=0}^{\infty} (\varphi'_n(a) - k_m^{(1)} \varphi_n(a)) B_{nm}^{(1)} = 0, \quad m = 1, 2, \dots, \tag{5.3b}$$

$$\sum_{n=0}^{\infty} (\varphi'_n(b) - ik_0^{(3)} \varphi_n(b)) B_{n0}^{(3)} = 0, \tag{5.3c}$$

$$\sum_{n=0}^{\infty} (\varphi'_n(b) + k_m^{(3)} \varphi_n(b)) B_{nm}^{(3)} = 0, \quad m = 1, 2, \dots, \tag{5.3d}$$

where $\|Z_0^{(1)}\|^2 = \langle Z_0^{(1)}, Z_0^{(1)} \rangle$, and the coefficients $B_{nm}^{(j)}$, $n, m = -1, 0, 1, 2, \dots, j = 1, 3$, are defined by

$$B_{nm}^{(j)} = \begin{cases} \langle Z_n(z; x = a), Z_m^{(1)}(z) \rangle, & j = 1, \\ \langle Z_n(z; x = b), Z_m^{(3)}(z) \rangle, & j = 3. \end{cases} \tag{5.3e}$$

The reflection and transmission coefficients (A_R, A_T) appearing in (2.6a, b), as well as the coefficients $\{C_n^{(1)}\}_{n \in \mathbb{N}}$ and $\{C_n^{(3)}\}_{n \in \mathbb{N}}$ controlling the dynamics in the two half-strips, are then, obtained in terms of $\varphi_n(a)$ and $\varphi_n(b)$, $n = 0, 1, 2, \dots$, as follows:

$$A_R = \left(\frac{\sum_{n=0}^{\infty} \varphi_n(a) B_{n0}^{(1)}}{\|Z_0^{(1)}\|^2} - \exp(ik_0^{(1)}a) \right) \exp(ik_0^{(1)}a),$$

$$C_m^{(1)} = \frac{\sum_{n=0}^{\infty} \varphi_n(a) B_{nm}^{(1)}}{\|Z_m^{(1)}\|^2}, \quad m = 1, 2, 3 \dots, \tag{5.4a}$$

and

$$A_T = \frac{\sum_{n=0}^{\infty} \varphi_n(b) B_{n0}^{(3)}}{\|Z_0^{(3)}\|^2} \exp(-ik_0^{(3)}b), \quad C_m^{(3)} = \frac{\sum_{n=0}^{\infty} \varphi_n(b) B_{nm}^{(3)}}{\|Z_m^{(3)}\|^2}, \quad m = 1, 2, 3 \dots \tag{5.4b}$$

Equations (5.4a) and (5.4b) are obtained, respectively, from the sixth and eighth terms of the variational equation (3.3).

In accordance with (4.7b), the sloping-bottom mode becomes identically zero in the vicinity of the end points $x \rightarrow a + 0$ and $x \rightarrow b - 0$, since we have assumed that $h'(x) = 0$ there. As a result, $\varphi_{-1}(x)$ does not appear in the boundary conditions (5.3a–e). However, some boundary conditions are also needed for $\varphi_{-1}(x)$ at $x = a$ and $x = b$. It turns out that the appropriate ones are

$$\varphi_{-1}(a) = \varphi'_{-1}(a) = 0, \quad \varphi_{-1}(b) = \varphi'_{-1}(b) = 0, \tag{5.5}$$

which are fully compatible with (4.7b).

Furthermore, from the last two terms on the left-hand side variational equation (3.3), we obtain the following edge conditions at the plate ends:

$$\frac{\partial^3 w}{\partial x^3} - (2 - \nu)q^2 \frac{\partial w}{\partial x} = 0 \quad \text{at } x = a \quad \text{and } x = b, \tag{5.6a}$$

$$\frac{\partial^2 w}{\partial x^2} - \nu q^2 w = 0 \quad \text{at } x = a \quad \text{and } x = b, \tag{5.6b}$$

which ensure that the elastic plate is free of shear force (5.6a) and moment (5.6b), respectively, at the ends $x = a$ and $x = b$.

Remarks: (i) Under the appropriate smoothness assumptions for the depth function $h(x)$ (e.g. $h(x)$ is two times continuously differentiable), all coefficients of the CMS are continuous functions of x and can be calculated in advance, by means of the solution of the local (vertical) eigenvalue problem (4.5b). (ii) The present model can be directly extended to treat more general floating structures characterized by variable flexural rigidity and mass parameters. (iii) Discontinuities of the physical parameters (depth function and its derivatives, flexural rigidity and mass distributions) can also be treated by introducing an appropriate domain decomposition and matching conditions at the points of the discontinuities.

5.2. The form of the CMS in constant depth

In areas where the depth is constant, $h(x) = h$, the CMS (5.1a, b) is greatly simplified. First, all terms associated with φ_{-1} can be dropped, since $\varphi_{-1} = 0$, when $h'(x) = 0$ (cf. (4.7b)). In addition, the coefficients of the CMS become constant and they are further simplified by dropping the terms containing x -derivatives in (5.2a–c). Then, the present CMS takes the form

$$\sum_{n=0}^{\infty} \langle Z_n, Z_m \rangle (\varphi_n''(x) + (\kappa_n^2 - q^2)\varphi_n(x)) - f_n \varphi_n(x) = i\omega w(x),$$

$$m = 0, 1, 2, 3 \dots, \quad (5.7a)$$

and

$$D \left(\frac{\partial^2}{\partial x^2} - q^2 \right)^2 w + (1 - \varepsilon)w = \frac{i\mu}{\omega} \sum_{n=0}^{\infty} \varphi_n(x), \quad (5.7b)$$

where

$$f_n = \kappa_n \tanh(\kappa_n h). \quad (5.8)$$

In (5.7a, b) and (5.8), $\{\kappa_n, Z_n(z), n = 0, 1, 2, 3 \dots\}$ are the eigenvalues and eigenfunctions given by (4.3a, b). The general solution of the present CMS (5.7a, b), is given by

$$\varphi_n(x) = \alpha_n \exp(iK_n x) + \beta_n \exp(-iK_n x), \quad n = 0, 1, 2, 3 \dots, \quad (5.9a)$$

and

$$w(x) = \frac{i}{\omega} \sum_{n=0}^{\infty} f_n \varphi_n(x), \quad (5.9b)$$

where α_n, β_n are constants and K_n are the values of the x -direction wavenumber of the hydroelastic problem,

$$K_n = \sqrt{\kappa_n^2 - q^2}. \quad (5.9c)$$

Indeed, direct substitution of (5.9a) in (5.7a) leads to (5.9b). Using the latter in (5.7b) we see that this equation is also satisfied, since all modes satisfy the hydroelastic dispersion relation, (4.3b).

It is now obvious that, in the case of constant depth, the solution of the present CMS exactly satisfies (4.4), rendering our system fully compatible with the models based on eigenfunction expansion techniques (e.g. Ertekin 1998; Takagi *et al.* 2000; Hong *et al.* 2003).

5.3. Shallow-water asymptotic form of the CMS

Assuming, in addition to constant depth, shallow water conditions ($\mu h \rightarrow 0$), and ignoring the evanescent modes ($\varphi_n(x) \approx 0, n \geq 3$), the dispersion relation (4.3b) implies $\kappa_n h \rightarrow 0, n = 0, 1, 2$. Then, using the asymptotics of $\tanh(\kappa h)$ for small argument, the dispersion relation takes the following asymptotic form:

$$\mu h \approx D\kappa_n^6 h^2 + (1 - \varepsilon)\kappa_n^2 h^2, \quad \kappa_n h \rightarrow 0, \quad n = 0, 1, 2. \quad (5.10)$$

In this case, the coefficients $f_n, n = 0, 1, 2$, (5.8), become

$$f_n = \kappa_n \tanh(\kappa_n h) \approx \kappa_n^2 h, \quad n = 0, 1, 2, \quad (5.11a)$$

and the corresponding vertical eigenfunctions $Z_n(z), n = 0, 1, 2$, defined by (4.3a), simplify to

$$Z_n(z) \approx 1, \text{ and thus } \langle Z_n, Z_m \rangle \approx h, \quad n, m = 0, 1, 2. \quad (5.11b)$$

Thus, in the shallow-water constant-depth case, the solution of the CMS is

$$\varphi(x, z) = \sum_{n=0}^{n=2} \varphi_n(x) Z_n(z) \approx \sum_{n=0}^{n=2} \varphi_n(x) = \sum_{n=0}^{n=2} \alpha_n \exp(iK_n x) + \beta_n \exp(-iK_n x), \quad (5.12)$$

where $K_n = \sqrt{\kappa_n^2 - q^2}$, $n=0, 1, 2$, and the constants κ_n , $n=0, 1, 2$, are obtained as the roots of the asymptotic dispersion relation (5.10).

The above results, in the case of normal incidence ($q=0$), are in perfect agreement with the ‘‘shallow-wave equation of a freely floating board’’ derived by Stoker (1967, §10.13, equation 10.13.74), which, in the present notation, reads as follows:

$$Dh \frac{d^6 \varphi(x)}{dx^6} + (1 - \varepsilon)h \frac{d^2 \varphi(x)}{dx^2} + \mu \varphi(x) = 0, \quad a < x < b. \quad (5.13)$$

The dispersion relation of (5.13) is exactly (5.10).

6. Numerical results and discussion

The discrete version of the CMS (5.1a, b) is obtained by truncating the local-mode series (4.6) to a finite number of terms (modes), and using central second-order finite differences to approximate the horizontal derivatives. Discrete boundary conditions are obtained by using second-order forward and backward differences to approximate the horizontal derivatives in (5.3a, d), (5.5) and (5.6a, b) at the ends $x=a$ and $x=b$. Thus, the discrete scheme obtained is uniformly of second order in the horizontal direction. The coefficient matrix of the discrete system is block structured with 3- and 5-diagonal blocks, corresponding to the discrete versions of (5.1a) and (5.1b), respectively. The system matrix has a total dimension $(N_m + 3)(N + 1)$, where N_m denotes the index where the series (4.6) is truncated and N is the number of segments subdividing the interval $a \leq x \leq b$.

(i) Floating elastic plate in constant depth

For comparison purposes, we first examine the hydroelastic behaviour of a thin elastic plate floating on a water layer of constant depth. The width of the plate is $L = b - a = 500$ m and its flexural rigidity is $D = 10^5$ m⁴ (per metre in the y -direction). The water depth is $h = 10$ m, and the incoming waves are normally incident ($\theta_1 = 0^\circ$). The effect of plate mass (which is of secondary importance) has been ignored in the computations ($\varepsilon = 0$). The frequency of the incoming wave is taken to be $\omega = 0.4$ rad s⁻¹, which implies that the depth-to-wavelength ratio is $h/\lambda = 0.066$ and the water can be considered to be approximately shallow. In this case (flat seabed), the sloping-bottom mode is zero (cf. (4.7b)), and our solution already converges on using only the first three modes $n=0, 1, 2$. Comparisons concerning the elastic-plate deflection normalized with respect to the waveheight ($|w|/H$), and the modulus of the wave potential on the plate ($|\varphi(x, z=0)|$), as obtained by the present CMS, using in total 5 modes and $N = 250$ segments, are presented in figure 3, against the predictions by Stoker’s shallow-wave model, (5.13). The two solutions exhibit the same behaviour and are in good agreement. The small differences (2%–3%) are attributed to the fact that the wave conditions are at the border between shallow and intermediate depth.

In the same case, the real and imaginary parts of the calculated wave field on the vertical (x, z)-plane, as obtained by the present CMS, are plotted in figure 4 by using equipotential lines. In order to better illustrate the results, each plot has been split into a sequence of (vertically arranged) subplots corresponding to horizontal segments of 150 m length. Also, in the same figure the free-surface elevation η in

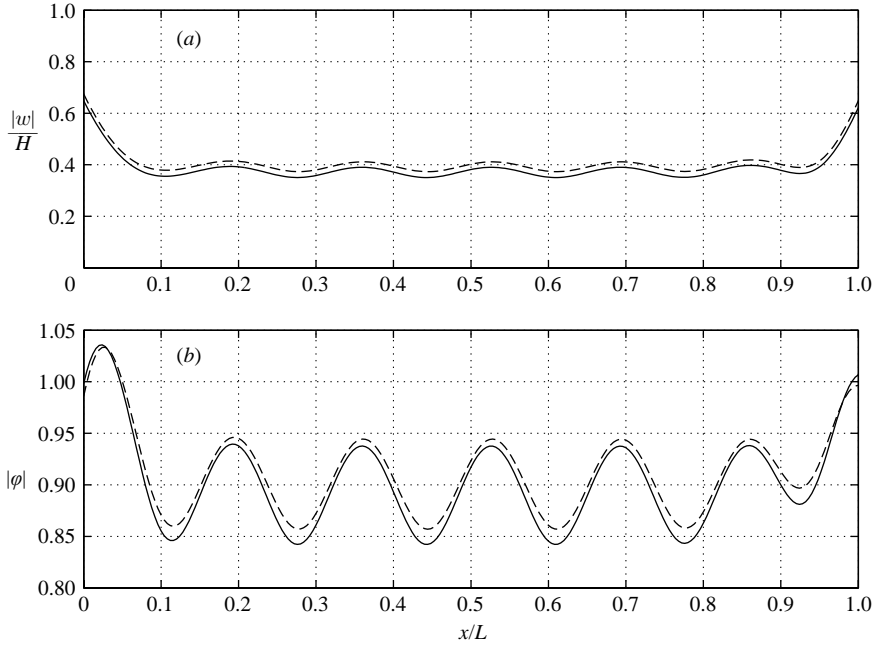


FIGURE 3. Comparison between the present CMS results (solid lines) and Stoker’s model (dashed lines), concerning (a) the modulus of the deflection and (b) the modulus of the wave potential on $z = 0$.

the neighbourhood of the elastic plate is shown by a thin line, and the elastic-plate deflection w by a thick line, respectively. We can clearly observe in this figure the good matching of the wave field on the vertical interfaces at $x = 0$ m and at $x = 500$ m, as achieved by using only 5 modes in the local-mode series representation.

A second case has also been examined, which corresponds to deep water conditions. This case, which refers to model scale, concerns an elastic plate of width $L = 1.4$ m, with flexural rigidity parameter $D = 1.74 \times 10^{-3} L^4$, in constant depth $h = 0.5$ m, subject to the action of normally incident waves ($\theta_1 = 0^\circ$), with angular frequency $\omega = 4\pi \text{ rad s}^{-1}$, and normalized wavelength $\lambda_1/L = 0.278$. The depth-to-wavelength ratio is $h/\lambda = 1.28$. In figure 5 the modulus of the normalized plate deflection with respect to the amplitude of the incoming wave ($2|w|/H$) is presented, as obtained by the present CMS (again with 5 modes and $N = 250$), and as obtained by Takagi *et al.* (2000, figure 4). The latter has been found to be in perfect agreement with the results of modal analysis by Yoshimoto *et al.* (1997), and with the results by Hermans (2003, figure 4). That is, the present CMS predictions agree very well with various existing well-established models, which, however, are limited to constant-depth environments.

(ii) *Elastic plate over a smooth underwater shoal*

In order to illustrate the effects of variable bathymetry (sloping bottom) on the hydroelastic behaviour of the system, we examine the same elastic plate as in the first constant-depth ($L = 500$ m, $D = 10^5 \text{ m}^4$, $\varepsilon = 0$) lying over a smooth underwater shoal, characterized by the following depth function:

$$h(x) = \frac{h_1 + h_3}{2} - \frac{h_1 - h_3}{2} \tanh\left(3\pi\left(\frac{x - a}{b - a} - \frac{1}{2}\right)\right), \quad a = 0 < x < b = 500 \text{ m.} \quad (6.1)$$

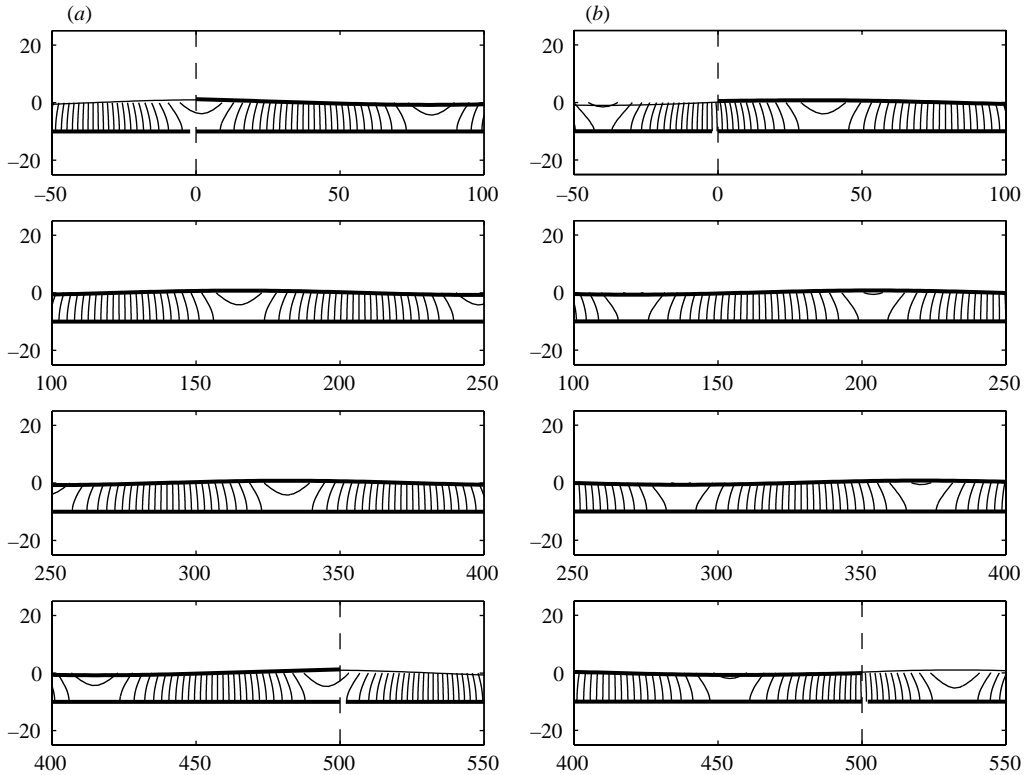


FIGURE 4. (a) Real and (b) imaginary parts of the calculated wave field, as obtained by the present method, in the case of constant depth. The elastic plate extends from $x=0$ m to $x=500$ m. The free-surface elevation is shown by a thin line and the elastic plate deflection by a thick line, respectively. The calculated values of the reflection and transmission coefficients as obtained by the present CMS are: $|A_R|=0.089$, $|A_T|=0.996$.

For comparison with the corresponding constant-depth case, the average depth of this bottom profile, $h_m = 0.5(h_1 + h_3)$, has been kept equal to 10 m, and the angular frequency of the incident wave is the same as before, $\omega = 0.4 \text{ rad s}^{-1}$.

Numerical results obtained by the present method are presented below, for two bottom profiles generated by (6.1). The first one is characterized by $h_1 = 12$ m, $h_3 = 8$ m and has maximum bottom slope $s_{\max} = 3.8\%$, while the second profile, characterized by $h_1 = 15$ m, $h_3 = 5$ m, is much steeper, $s_{\max} = 9.4\%$.

The real and imaginary parts of the calculated wave field, as obtained by the present CMS using in total again 5 modes and 250 segments (which has been proved enough for numerical convergence), are shown in figures 6 and 7, for the two profiles. The extension of the equipotential lines below the bottom surface (as calculated by means of (4.6)) has been maintained in the above figures in order to better visualise the fulfilment of the bottom boundary condition. Also, in these figures, the free-surface elevation in the neighbourhood of the elastic plate and the plate deflection are shown, using thin and thick lines, respectively. In all cases we observe that the matching of the wave field on the vertical interfaces, at the ends of the plate ($x=0$ m and at $x=500$ m), indicated by vertical dashed lines, is excellent. Moreover, we observe that the equipotential lines intersect the bottom surface perpendicularly, as they ought, because of the Neumann boundary condition, both on the horizontal and on the

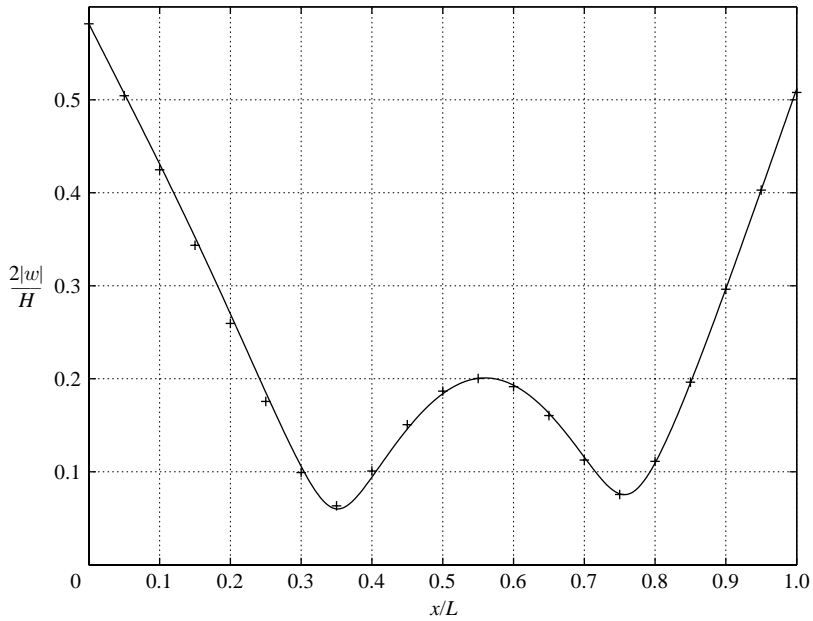


FIGURE 5. Comparison between present method (solid lines) and Takagi *et al.*'s (2000) results (crosses), for the modulus of the elastic-plate deflection normalized with respect to the normally incident wave amplitude.

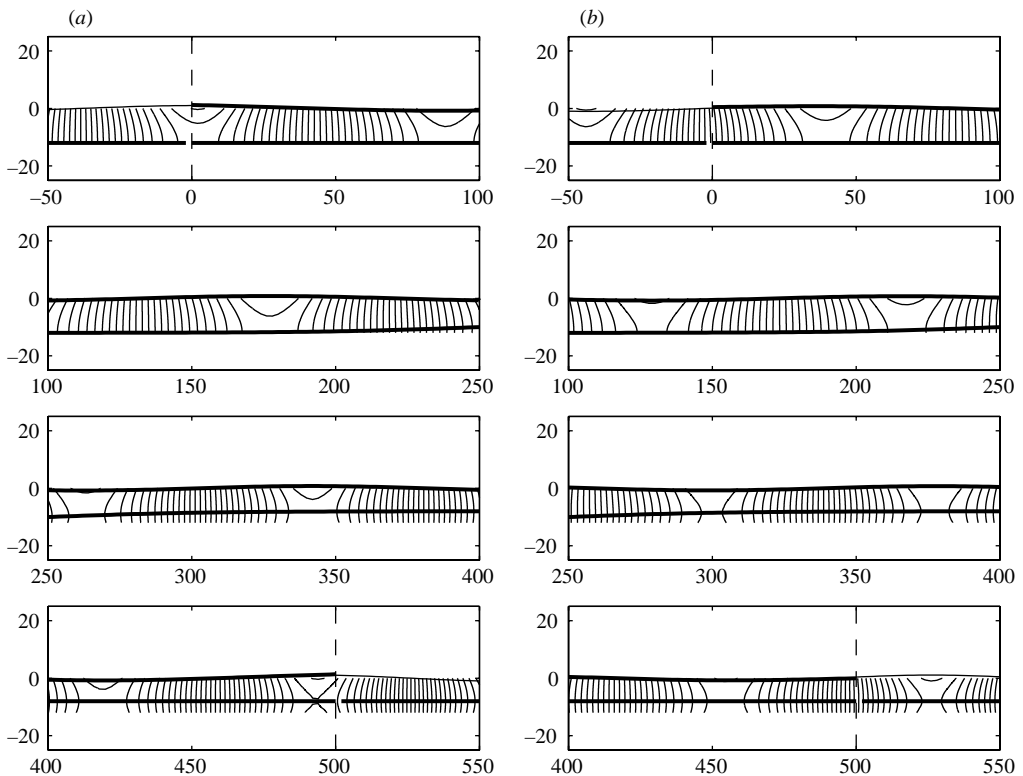


FIGURE 6. Same as figure 4, but for the case of an elastic plate over the shoal characterized by the depth profile (6.1) with $h_1 = 12$ m and $h_3 = 8$ m (maximum bottom slope 3.8 %).

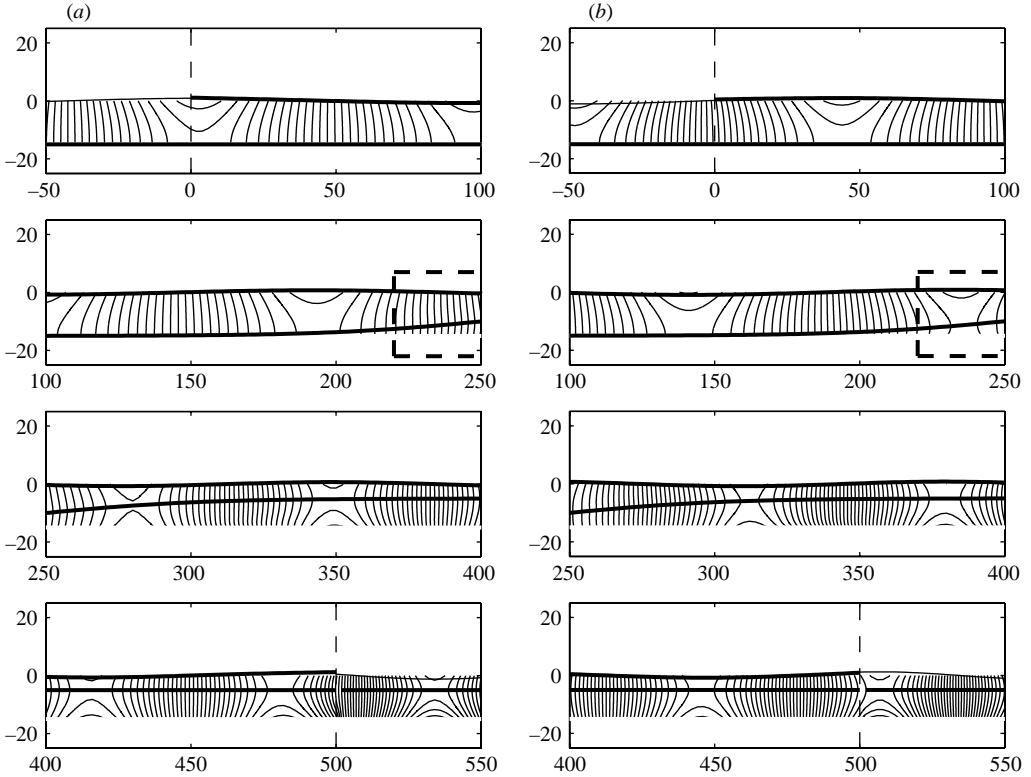


FIGURE 7. Same as figure 4, but for the case of an elastic plate over the shoal characterized by the depth profile (6.1) with $h_1 = 15$ m and $h_3 = 5$ m (maximum bottom slope 9.4 %).

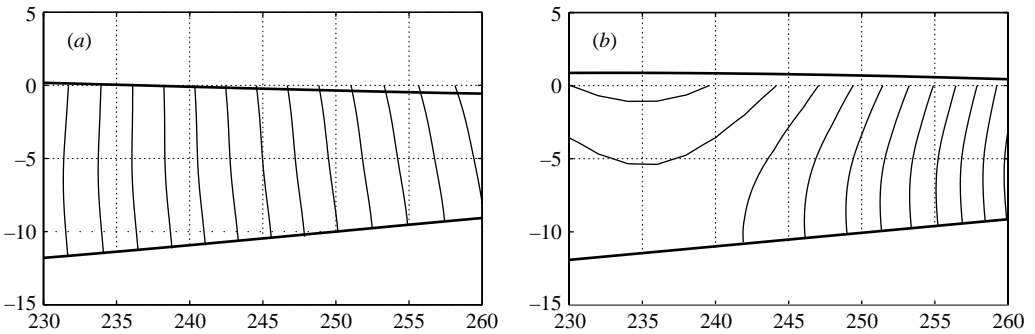


FIGURE 8. (a, b) Close-up of the wave field in the local area shown by dashed lines in figures 7(a) and (b), respectively, where the local bottom slope is maximum.

sloping parts of the bottom. This fact is better illustrated in the case of the steeper bottom profile with the aid of the close-ups of the local area shown in figure 8.

In figure 9 the moduli of the modal-amplitude functions, i.e. the quantities $|\varphi_n(x)|$ in $a \leq x \leq b$, are plotted, as obtained by the present method. The horizontal axis in figure 9 is a multiple repetition of the interval $[a, b]$, i.e. a sequence of repeated intervals $[a, b]$, each associated with a mode and named after the mode number. In the n th replica of $[a, b]$ the amplitudes $|\varphi_n(x)|$ of the n th mode, are plotted, using solid, lines, respectively. Also, in the same figure, the curve $0.1(n - 2)^{-4}$ is drawn, bounding the

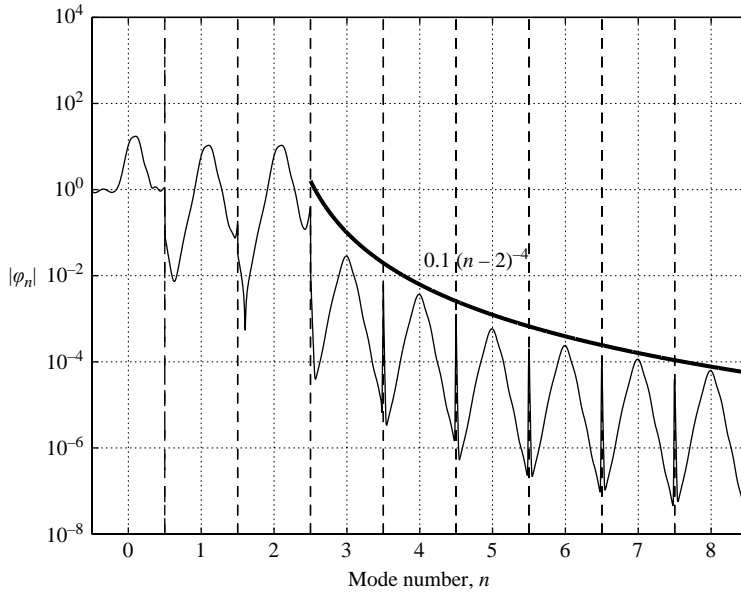


FIGURE 9. Moduli of the modal-amplitude functions $|\varphi_n(x)|$ vs. $x \in [a, b]$ in the variable bathymetry region, for various modes $n = -1, 0, 1, 2, \dots$. Environment and wave conditions as in figure 7. The curve $0.1(n - 2)^{-4}$, shown by using a thick solid line, bounds the maxima of the modal amplitudes of all potentials.

maxima of the amplitudes of all modal functions. On the basis of these (and many other similar) results, we can conjecture that the decay of the modal amplitudes is of $O(n^{-4})$, which is sufficient to ensure the uniform convergence (up to and including the boundaries) of the corresponding local-mode series and their derivatives.

In figure 10, the effect of the bottom slope on the modulus of the elastic-plate deflection ($|w|/H$) is presented. We observe in this figure that, in the mean, the elastic deflection increases significantly at the front part ($x/L < 0.5$) of the plate as the shoal becomes steeper. This result is justified by the higher hydroelastic excitation by waves in the front (upwave) elastic-plate part, which is induced by the extra reflected energy from the shoal. On the other hand, the absolute maximum of the plate deflection in the vicinity of the front edge ($x = 0$) tends to slightly decrease.

In figure 11, the effect of the incident wave angle on the modulus of the elastic plate deflection is presented. In this case, results are shown for the 9.4 % sloping bottom profile. The flexural rigidity and the rest parameters of the plate have been kept the same ($D = 10^5 \text{ m}^4$, $\varepsilon = 0$), and Poisson's ratio is taken to be $\nu = 0.25$. The numerical results are again based on the present CMS using 5 modes and 250 segments to discretize the interval $a \leq x \leq b$. We can observe in figure 11 that, as the incident wave angle increases, the elastic plate deflection at the front (upwave) part ($x/L < 0.5$) of the plate also increases, while at the back (downwave) part it becomes smaller. As the incident wave angle increases, the horizontal (along the x -axis) wavelength of the wave and of the plate deflection increase, as they ought. Also, refraction phenomena (which are absent in the normal incidence case) come into play and become more and more significant. The values of the calculated reflection and transmission coefficients for all the above cases are compared in table 1, and are found to satisfy the energy conservation relation, (2.4).

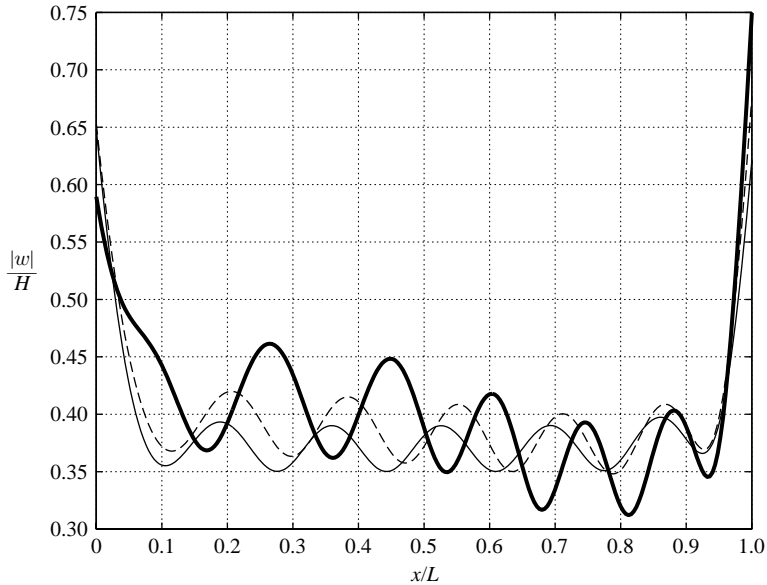


FIGURE 10. Effect of the bottom profile on the modulus of the elastic-plate deflection. The three bottom profiles examined are: (i) horizontal bottom (thin solid line), (ii) 3.8% sloping bottom (dashed line), (iii) 9.4% sloping bottom (thick solid line).

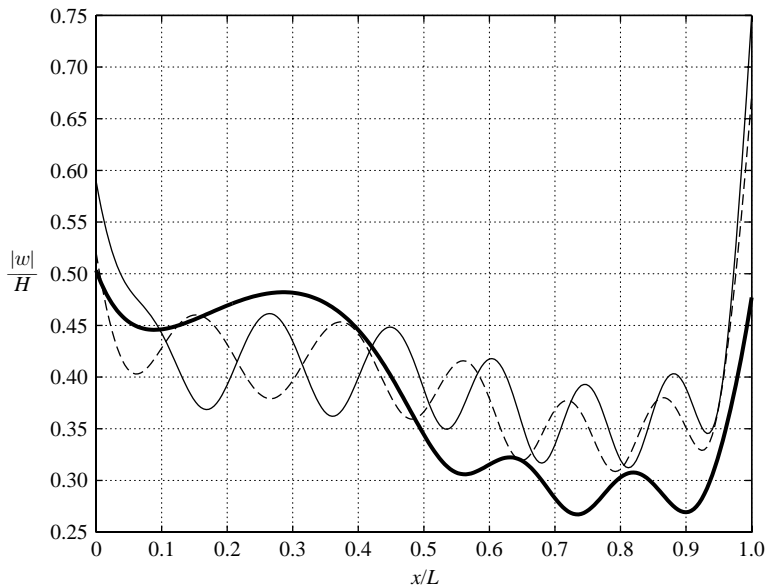


FIGURE 11. Effect of the incident wave angle on the modulus of the elastic-plate deflection for an elastic plate over a shoal (maximum bottom slope 9.4%). The three incidence angles examined are: (i) normal incidence, $\theta_1 = 0^\circ$ (thin solid line), (ii) oblique incidence, $\theta_1 = 30^\circ$ (dashed line), and (iii) very oblique incidence, $\theta_1 = 60^\circ$ (thick solid line).

(iii) *Elastic plate over smooth undulating bottom*

Finally, in order to present the effects of bottom corrugations on the hydroelastic behaviour of the system, we examine the same configuration (elastic plate $L = 500$ m,

Bottom type:	Flat bottom	Sloping 3.8 %	Sloping 9.4 %	Sloping 9.4 %	Sloping 9.4 %
Wave incidence:	$\theta_1 = 0^\circ$	$\theta_1 = 0^\circ$	$\theta_1 = 0^\circ$	$\theta_1 = 30^\circ$	$\theta_1 = 60^\circ$
$ A_R $	0.089	0.100	0.145	0.094	0.045
$ A_T $	0.996	1.082	1.249	1.197	0.963

TABLE 1. Calculated values of the wave reflection $|A_R|$ and transmission $|A_T|$ coefficients in the case of a floating elastic plate over a shoal, for the various profiles and incidence angles.

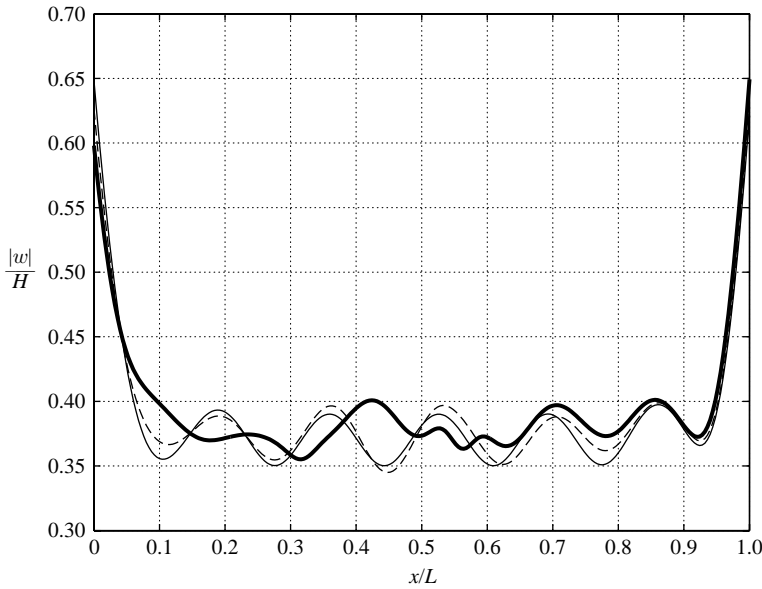


FIGURE 12. Effect of bottom corrugations on the modulus of the elastic-plate deflection. The three bottom profiles examined are: (i) horizontal bottom (thin solid line), (ii) undulating bottom with $A_b/h = 15\%$ (dashed line), (iii) undulating bottom with $A_b/h = 30\%$ (thick solid line).

$D = 10^5 \text{ m}^4$, $\varepsilon = 0$) but lying over a smooth undulating bottom. In this case, the bottom profile is taken to be defined by the following depth function:

$$h(x) = h - g(x)A_b \sin(k_b(x - a)), \quad a = 0 < x < b = 500 \text{ m}, \quad (6.2a)$$

where $k_b = 2\pi/\lambda_b$ is the bottom wavenumber, λ_b is the corresponding wavelength, and A_b is the amplitude of bottom undulations. The function $g(x)$ used in (6.2a) is a filter function defined by

$$g(x) = \left(1 - \exp\left(-\left(\frac{x-a}{\lambda_b}\right)^2\right)\right) \left(1 - \exp\left(-\left(\frac{x-b}{\lambda_b}\right)^2\right)\right). \quad (6.2b)$$

The above function has essential support in $a < x < b$, and its value along with its derivative become zero at both ends $x = a$ and $x = b$ of the plate. For comparison with the previous (constant-depth and shoal) cases, the average depth of the bottom profile has been kept the same ($h = 10 \text{ m}$), as has the frequency of the normally ($\theta_1 = 0^\circ$) incident wave, $\omega = 0.4 \text{ rad s}^{-1}$.

Numerical results are presented in figure 12, for two bottom profiles generated by (6.2a, b) using $L/\lambda_b = 4$, in comparison with the deflection of the same elastic plate

in the case of the horizontal bottom. The first undulating bottom is characterized by $A_b/h = 15\%$ and has maximum bottom slope $s_{\max} = 7.5\%$ and curvature 0.0036 m^{-1} , while the second profile, characterized by $A_b/h = 30\%$, is much steeper, having maximum bottom slope $s_{\max} = 15\%$ and curvature 0.0072 m^{-1} . In this particular case, the calculated reflection and transmission coefficients, as well as the average values of the elastic-plate deflection, do not significantly change, compared to the flat bottom case. On the other hand, we observe in figure 12 that, as the amplitude of bottom undulations increases, the shape of the elastic-plate deflection (modulus) becomes more complex in the middle part of the plate, which lies exactly above the region where the bottom undulations are stronger.

7. Conclusions

A new coupled-mode model has been derived and applied to the hydroelastic analysis of large floating bodies of shallow draught, lying over variable bathymetry regions. Under the assumption of small-amplitude incident waves and small body deflections, the linearised water-wave equations and thin-elastic-plate theory have been used. The present approach is based on appropriate extension of the consistent coupled-mode model developed by Athanassoulis & Belibassakis (1999), for waves propagating in variable bathymetry regions. In its present form our method can also find useful applications to problems concerning water-wave interaction with ice sheets of small and uniform thickness, lying over variable bathymetry.

The present method does not introduce any simplifying assumptions or other restrictions concerning either the bottom slope and curvature, or the vertical structure of the wave field. All wave phenomena are linearly fully modelled and, thus, the present method can serve as a useful tool for the analysis of the hydroelastic behaviour of the system in the whole range of parameters, within the regime of linear theory. An important feature of the numerical solution of the problem by means of the enhanced local-mode series representation is that it exhibits rapid convergence, corresponding to the fast decay of the modal amplitudes $|\varphi_n| = O(n^{-4})$. Thus, a small number of modes (of the order of 5 to 6) retained in the local-mode series suffices to obtain accurate results.

The present method can be easily extended to the fully three-dimensional hydroelastic problem over a general seafloor, including bodies or structures characterized by variable thickness (draught), flexural rigidity and mass distributions. Finally, the analytical structure of the present model facilitates its extension to the modelling and analysis of weakly nonlinear (second and higher order) wave-elastic floating structure-seabed interactions in variable bathymetry regions.

The authors are indebted to the anonymous referees for their constructive comments and suggestions which helped them in improving the presentation of the coupled-mode system and motivated the additional results given in the Appendix.

Appendix. Relation between the present functional F and the standard energy functional of thin-plate theory

We shall now show that, under the assumptions made in our analysis, i.e. time-harmonic dependence and y -periodicity, the variational principle obtained by means

of the following part of our functional F (defined by (3.1)):

$$\begin{aligned}
 F_1 &= -\frac{\omega^2 D}{2} \int_{x=a}^{x=b} \left(\left(\frac{\partial^2 w}{\partial x^2} \right)^2 + 2q^2 \left(\frac{\partial w}{\partial x} \right)^2 + \left(q^4 - \frac{\varepsilon}{D} \right) w^2 \right) dx + \nu \omega^2 D q^2 \left[w \frac{\partial w}{\partial x} \right]_{x=a}^{x=b} \\
 &= \frac{\omega^2}{2\rho g} \left\{ - \int_{x=a}^{x=b} \left(D \left\{ \left(\frac{\partial^2 w}{\partial x^2} \right)^2 + 2q^2 \left(\frac{\partial w}{\partial x} \right)^2 + q^4 w^2 \right\} - m \omega^2 w^2 \right) dx \right. \\
 &\quad \left. + 2\nu D q^2 \left[w \frac{\partial w}{\partial x} \right]_{x=a}^{x=b} \right\}, \tag{A 1}
 \end{aligned}$$

is equivalent to the variational principle based on the standard energy functional of thin-plate theory, defined as the difference between the strain energy and the kinetic energy of the elastic plate (in vacuo):

$$\begin{aligned}
 F_2 &= \frac{1}{2} \int_t dt \int_y dy \int_{x=a}^{x=b} dx \left\{ \left(D \left(\frac{\partial^2 \tilde{w}}{\partial x^2} + \frac{\partial^2 \tilde{w}}{\partial y^2} \right)^2 \right. \right. \\
 &\quad \left. \left. - 2(1-\nu) \left(\frac{\partial^2 \tilde{w}}{\partial x^2} \frac{\partial^2 \tilde{w}}{\partial y^2} - \left(\frac{\partial^2 \tilde{w}}{\partial x \partial y} \right)^2 \right) - m \left(\frac{\partial \tilde{w}}{\partial t} \right)^2 \right) \right\}. \tag{A 2}
 \end{aligned}$$

The real-valued field $\tilde{w} = \tilde{w}(x, y, t)$, appearing in (A 2), is the plate deflection in the time domain, while the field $w = w(x; \omega) = w_R(x; \omega) + i w_I(x; \omega)$, appearing in (A 1) and in the main part of the present paper, is a complex-valued deflection field, related to the former by the relation

$$\tilde{w} = \tilde{w}(x, y, t) = \text{Re}\{w(x; \omega) \exp(i(qy - \omega t))\}, \tag{A 3}$$

cf. (2.1c). In order to establish the equivalence between the variational principle obtained by (A 1) and the usual variational principle obtained by (A 2) (for the time-harmonic, oblique-incidence problem), use will be made of the following identities:

$$\begin{aligned}
 2 \int_y dy \int_{x=a}^{x=b} \left(\frac{\partial^2 \tilde{w}}{\partial x^2} + \frac{\partial^2 \tilde{w}}{\partial y^2} \right)^2 dx &= \text{Re} \int_y e^{2i(qy - \omega t)} dy \int_{x=a}^{x=b} \left(\frac{\partial^2 w}{\partial x^2} - q^2 w \right)^2 dx \\
 &\quad + \text{Re} \int_y dy \int_{x=a}^{x=b} \left| \frac{\partial^2 w}{\partial x^2} - q^2 w \right|^2 dx, \tag{A 4a}
 \end{aligned}$$

$$\begin{aligned}
 2 \int_y dy \int_{x=a}^{x=b} \frac{\partial^2 \tilde{w}}{\partial x^2} \frac{\partial^2 \tilde{w}}{\partial y^2} dx &= -q^2 \text{Re} \int_y e^{2i(qy - \omega t)} dy \int_{x=a}^{x=b} \left(w \frac{\partial^2 w}{\partial x^2} \right) dx \\
 &\quad - \text{Re} \int_y dy \int_{x=a}^{x=b} q^2 \frac{\partial^2 w}{\partial x^2} \bar{w} dx, \tag{A 4b}
 \end{aligned}$$

$$\begin{aligned}
 2 \int_y dy \int_{x=a}^{x=b} \left(\frac{\partial^2 \tilde{w}}{\partial x \partial y} \right)^2 dx &= -q^2 \text{Re} \int_y e^{2i(qy - \omega t)} dy \int_{x=a}^{x=b} \left(\frac{\partial w}{\partial x} \right)^2 dx \\
 &\quad + \text{Re} \int_y dy \int_{x=a}^{x=b} q^2 \left| \frac{\partial w}{\partial x} \right|^2 dx, \tag{A 4c}
 \end{aligned}$$

and

$$\begin{aligned}
 2 \int_y dy \int_{x=a}^{x=b} \left(\frac{\partial \tilde{w}}{\partial t} \right)^2 dx &= -\omega^2 \text{Re} \int_y e^{2i(qy - \omega t)} dy \int_{x=a}^{x=b} w^2 dx \\
 &\quad + \omega^2 \text{Re} \int_y dy \int_{x=a}^{x=b} |w|^2 dx. \tag{A 4d}
 \end{aligned}$$

In deriving (A 4), we have made use of the definition (A 3) and the equation

$$2 \operatorname{Re}(z_1) \operatorname{Re}(z_2) = \operatorname{Re}(z_1 z_2) + \operatorname{Re}(z_1 \bar{z}_2), \tag{A 5}$$

which is valid for any two complex numbers z_1, z_2 . Here and in what follows an overbar denotes the complex conjugate.

Consider now (A 4a), and apply time integration to both sides of it:

$$2 \int_t dt \int_y dy \int_{x=a}^{x=b} \left(\frac{\partial^2 \tilde{w}}{\partial x^2} + \frac{\partial^2 \tilde{w}}{\partial y^2} \right)^2 dx = \operatorname{Re} \int_t dt \int_y e^{2i(qy - \omega t)} dy \int_{x=a}^{x=b} \left(\frac{\partial^2 w}{\partial x^2} - q^2 w \right)^2 dx + \text{second term.}$$

The quantity

$$\int_{x=a}^{x=b} \left(\frac{\partial^2 w}{\partial x^2} - q^2 w \right)^2 dx$$

is independent of t and y (remember that $w = w(x; \omega)$), thus the t - and y -integration applies only to $\exp(2i(qy - \omega t))$. Performing the t -integration over one time period and the y -integration over one periodic cell (of length $2\pi/q = 2\pi/\kappa_0^{(1)} \sin \theta_1$), we obtain

$$\int_t dt \int_y e^{2i(qy - \omega t)} dy = 0.$$

Similarly, we find that the first terms on the right-hand side of (A 4b, c, d) are zero, and thus, we obtain

$$F_2 = \frac{\pi^2}{\omega q} \operatorname{Re} \int_{x=a}^{x=b} dx \left\{ D \left(\left| \frac{\partial^2 w}{\partial x^2} - q^2 w \right|^2 + 2(1 - \nu) \left(q^2 \left(\frac{\partial^2 w}{\partial x^2} \bar{w} \right) + q^2 \left| \frac{\partial w}{\partial x} \right|^2 \right) - m\omega^2 |w|^2 \right) \right\}. \tag{A 6}$$

Using again formula (A 5) in the above equation, we obtain

$$F_2 = -\frac{\pi^2}{\omega q} \operatorname{Re} \int_{x=a}^{x=b} dx \left(D \left\{ \left(\frac{\partial^2 w}{\partial x^2} - q^2 w \right)^2 + 2(1 - \nu) q^2 \left(\left(\frac{\partial^2 w}{\partial x^2} w \right) + q^2 \left(\frac{\partial w}{\partial x} \right)^2 \right) \right\} - m\omega^2 w^2 \right) + \frac{2\pi^2}{\omega q} \int_{x=a}^{x=b} dx \left(D \left\{ \left(\frac{\partial^2 w_R}{\partial x^2} - q^2 w_R \right)^2 + 2(1 - \nu) q^2 \left(\left(\frac{\partial^2 w_R}{\partial x^2} w_R \right) + q^2 \left(\frac{\partial w_R}{\partial x} \right)^2 \right) \right\} - m\omega^2 w_R^2 \right). \tag{A 7}$$

Expanding the term in the curly brackets on the right-hand side of (A 7), and applying integration by parts to the terms

$$-2q^2 \nu \left(\frac{\partial^2 w}{\partial x^2} w + \left(\frac{\partial w}{\partial x} \right)^2 \right) \quad \text{and} \quad -2q^2 \nu \left(\frac{\partial^2 w_R}{\partial x^2} w_R + \left(\frac{\partial w_R}{\partial x} \right)^2 \right),$$

we finally obtain

$$\begin{aligned}
 F_2 &= F_{21} + F_{22} \\
 &= \frac{\pi^2}{\omega q} \operatorname{Re} \left(- \int_{x=a}^{x=b} \left(D \left\{ \left(\frac{\partial^2 w}{\partial x^2} \right)^2 + 2q^2 \left(\frac{\partial w}{\partial x} \right)^2 + q^4 w^2 \right\} - m\omega^2 w^2 \right) dx \right. \\
 &\quad \left. + 2\nu q^2 \left[w \frac{\partial w}{\partial x} \right]_{x=a}^{x=b} \right) + \frac{2\pi^2}{\omega q} \int_{x=a}^{x=b} \left(D \left\{ \left(\frac{\partial^2 w_R}{\partial x^2} \right)^2 + 2q^2 \left(\frac{\partial w_R}{\partial x} \right)^2 + q^4 w_R^2 \right\} \right. \\
 &\quad \left. - m\omega^2 w_R^2 \right) dx + 2\nu q^2 \left[w_R \frac{\partial w_R}{\partial x} \right]_{x=a}^{x=b}. \tag{A 8}
 \end{aligned}$$

By comparing (A 1) and (A 8) it can be seen that the solution w_* of the variational equation $\delta F_1(w_*) = 0$, for any complex variation $\delta w = \delta w_R + i\delta w_I$, also satisfies $\delta F_2 = \delta F_{21} + \delta F_{22} = 0$. For, by first restricting δw to be $\delta w = \delta w_R + i0$ and using it in $\delta F_1(w_*) = 0$, we obtain $\delta F_{22}(w_*) = 0$. Consequently, for any admissible complex variation δw , we obtain

$$\delta F_2(w_*) = \delta F_{21}(w_*) = c \operatorname{Re}(\delta F_1(w_*)), \tag{A 9}$$

where c is a constant. Therefore, the stationarity of (the part F_1 of) our functional also guarantees the stationarity of the strain–kinetic energy functional (F_2) of thin-plate theory.

REFERENCES

- ANDRIANOV, A. I. & HERMANS, A. J. 2003 The influence of water depth on the hydroelastic response of a very large floating platform. *Mar. Struct.* **16**, 355–371.
- ATHANASSOULIS, G. A. & BELIBASSAKIS, K. A. 1999 A consistent coupled-mode theory for the propagation of small-amplitude water waves over variable bathymetry regions. *J. Fluid Mech.* **389**, 275–301.
- ATHANASSOULIS, G. A. & BELIBASSAKIS, K. A. 2002 A coupled-mode, fully-dispersive, weakly-nonlinear model for water waves over a general bathymetry. *Proc. 12th Intl Offshore and Polar Conference and Exhibition ISOPE 2002* (ed. J. S. Chung *et al.*), Kitakyushu, Japan, vol. 3, pp. 248–255.
- BALMFORTH, N. J. & CRASTER, R. V. 1999 Ocean waves and ice sheets. *J. Fluid Mech.* **395**, 89–124.
- BELIBASSAKIS, K. A., ATHANASSOULIS, G. A. & GEROSTATHIS T. P. 2001 A coupled-mode model for the refraction-diffraction of linear waves over steep three-dimensional bathymetry. *Appl. Ocean Res.* **23**, 319–336.
- BISHOP, R. E. D., PRICE, W. G. & WU, Y. S. 1986 A general linear hydroelasticity theory of floating structures. *Phil. Trans. R. Soc. Lond. A* **316**, 375–426.
- EATOCK TAYLOR, R. & OHKUSU, M. (Eds.) 2000 *J. Fluids Struct. Special issue* **14**, No. 7, October 2000.
- EATOCK TAYLOR, R. & WAITE, J. B. 1978 The dynamics of offshore structures evaluated by boundary integral techniques. *Intl J. Numer. Meth. Engng* **13**, 73–92.
- ERTEKIN, R. C. & KIM, J. W. 1999 Hydroelastic response of a floating mat-type structure in oblique shallow-water waves. *J. Ship Res.* **43**, 241–254.
- ERTEKIN, R. C., KIM, J. W., YOSHIDA, K. & MANSOUR, A. E. (Eds.) 2000 Hydroelastic response of a floating mat-type structure in oblique shallow-water waves. *Mar. Struct. Special issue* **13**, Nos. 4, 5.
- ERTEKIN, R. C., KIM, J. W., YOSHIDA, K. & MANSOUR, A. E. (Eds.) 2001 Hydroelastic response of a floating mat-type structure in oblique shallow-water waves. *Mar. Struct. Special Issue* **14**, Nos. 1, 2.
- EVANS, D. V. & PORTER, R. 2003 Wave scattering by narrow cracks in ice sheets floating on water of finite depth. *J. Fluid Mech.* **484**, 143–165.

- FALTINSEN, O. M. 2001 Hydroelastic slamming. *J. Mar. Sci. Technol.* **5** (2), 49–65.
- GRECO, M., LANDRINI, M. & FALTINSEN, O. M. 2003 Local hydroelastic analysis of VLFS with shallow draft. *Hydroelasticity in Marine Technology 2003*, Oxford, UK (ed. R. Exttock Taylor).
- HERMANS, A. J. 2000 A boundary element method for the interaction of free-surface waves with a very large floating flexible platform. *J. Fluids Struct.* **14**, 943–956.
- HERMANS, A. J. 2003 The ray method for the deflection of a floating flexible platform in short waves. *J. Fluids Struct.* **17**, 593–602.
- HONG, S. Y., CHOI, Y. R. & HONG, S. W. 2001 Investigation of draft effects on the analysis of hydroelastic responses of pontoon type VLFS. *Proc. 11th Intl Offshore and Polar Conference and Exhibition Conference ISOPE 2001* (ed. J. S. Chung *et al.*), vol. 1, pp. 222–228.
- HONG, S. Y., KIM, J. W., ERTEKIN, R. C. & SHIN, Y. S. 2003 An eigenfunction expansion method for hydroelastic analysis of a floating runway. *Proc. 13th Intl Offshore and Polar Conference and Exhibition Conference ISOPE 2003* (ed. J. S. Chung *et al.*), vol. 1, pp. 121–128.
- KASHIWAGI, M. 1998 A B-spline Galerkin scheme for calculating the hydroelastic response of a very large structure in waves. *J. Mar. Sci. Technol.* **3**, 37–49.
- KASHIWAGI, M. 2000 Research on hydroelastic responses of VLFS: recent progress and future work. *J. Offshore Polar Engng* **10**, 81–90.
- KIM, J. W. & ERTEKIN, R. C. 1998 An eigenfunction expansion method for predicting hydroelastic behavior of a shallow-draft VLFS. *Hydroelasticity in Marine Technology*, pp. 47–59 (ed. M. Kashiwagi *et al.*). RIAM, Kyushu University, Fukuoka, Japan.
- KIM, J. W. & ERTEKIN, R. C. 2002 Hydroelasticity of an infinitely long plate in oblique waves: linear Green Naghdi theory. *J. Engng Mari. Environ* **216**(M2), 179–197.
- KIRBY, J. T. & DALRYMPLE, R. A. 1983 Propagation of obliquely incident water waves over a trench. *J. Fluid Mech.* **133**, 47–63.
- LINTON, C. M. & CHUNG, H. 2003 Ocean waves and ice sheets. *Wave Motion* **38**, 43–52.
- LUKE, J. C. 1967 A variational principle for a fluid with a free surface. *J. Fluid Mech.* **27**, 395–397.
- MAGRAB, E. B. 1979 *Vibrations of Elastic Structural Members*. Sijthoff & Noordhoff, The Netherlands.
- MARCHENKO, A. V. & SHRIRA, V. I. 1991 Theory of two-dimensional nonlinear waves in liquid covered by ice. *Izve. Acad. Nauk SSSR, Mekh. Zhid. I Gaza* **4**, 125–133.
- MASSEL, S. 1989 *Hydrodynamics of Coastal Zones*. Elsevier.
- MASSEL, S. 1993 Extended refraction-diffraction equations for surface waves. *Coastal Engng* **19**, 97–126.
- MEI, C. C. 1983 *The Applied Dynamics of Ocean Surface Waves*. John Wiley & Sons (2nd Reprint, 1994, World Scientific).
- MEYLAN, M. H. 2001 A variational equation for the wave forcing of floating thin plates. *Appl. Ocean Res.* **23**, 195–206.
- MEYLAN, M. & SQUIRE, V. A. 1994 The response of ice floes to ocean waves. *J. Geophys. Res.* **99**, C1, 891–900.
- MURAI, M., INOUE, Y. & NAKAMURA, T. 2003 The prediction method of hydroelastic response of VLFS with sea bottom topographical effects. *Proc. 13th ISOPE Conference* (ed. J. S. Chung *et al.*), pp. 107–112.
- NAGATA, S., NIIZATO, H. & ISSHIKI, H. 2003 Variational principles related to motions of an elastic floating plate in nonlinear water wave. *Proc. 12th Intl Offshore and Polar Conference and Exhibition Conference ISOPE 2002* (ed. J. S. Chung *et al.*), vol. 1, pp. 350–357.
- NEWMAN, J. N. 1994 Wave effects on deformable bodies. *Appl. Ocean Res.* **16**, 47–59.
- OHKUSU, M. & NAMBA, Y. 1996 Analysis of hydroelastic behavior of a large floating platform of thin plate configuration in waves. *Proc. Intl Workshop on Very Large Floating Structures, Hayama, Japan*, pp. 143–148.
- PORTER, D. & PORTER, R. 2004 Approximations to wave scattering by an ice sheet of variable thickness over undulating bed topography. *J. Fluid Mech.* **509**, 145–179.
- SHIRAISHI S., IJIMA, K. & YONEYAMA, H. 2002 Elastic response of a very large floating structure in waves moored inside a coastal reef. *Proc. 12th Intl Offshore and Polar Conference and Exhibition Conference ISOPE 2002* (ed. J. S. Chung *et al.*), vol. 1, pp. 327–334.
- SQUIRE, V. A., DUGAN, J. P., WADHAMS, P., ROTTIER, P. J. & LIU, A. K. 1995 Of ocean waves and ice sheets. *Annu. Rev. Fluid Mech.* **27**, 115–168.
- STOKER J. J. 1957 *Water Waves: The Mathematical Theory with Applications*. Interscience.

- TAKAGI, K., SHIMADA, K. & IKEBUCHI, T. 2000 An anti-motion device for a very large floating structure. *Mari. Struct.* **13**, 421–436.
- TKACHEVA, L. A. 2001 Hydroelastic behaviour of a floating plate in waves. *J. Appl. Mech. Tech. Phys.* **42**, 991–996.
- WATANABE, E., UTSUNOMIYA T. & WANG, C. M. 2004 Hydroelastic analysis of pontoon-type VLFS: a literature survey. *Engng Struct.* **26**, 245–256.
- WEHAUSEN, J. N. & LAITONE, E. V. 1960 *Surface Waves*. Handbuch der Physik. Springer.
- WU, C., WATANABE, E. & UTSUNOMIYA, T. 1995 An eigenfunction matching method for analyzing the wave induced responses of an elastic floating plate. *Appl. Ocean Res.* **17**, 301–310.
- UTSUNOMIYA, T., WATANABE, E. & NISHIMURA, N. 2001 Fast multipole algorithm for wave diffraction/radiation problems and its application to VLFS in variable water depth and topography. *Proc. 12th Intl Conf. Offshore Mech. & Arctic Eng. OMAE 2001*, Paper 5202, vol. 7, pp. 1–7.
- YOSHIMOTO, M., HOSHINO, K., OHMATSU, S. & IKEBUCHI T. 1997 Slamming load acting on a very large floating structure with shallow draft. *J. Mar. Sci. Technol.* 37–46.
- ZAKHAROV, V. E. 1968 Stability of periodic waves of finite amplitude on a surface of a deep fluid. *J. Appl. Mech. Tech. Phys.* **9**(2), 190–194.